Turkish Journal of Earth Sciences (Turkish J. Earth Sci.), Vol. 19, 2010, pp. 101–122. Copyright ©TÜBİTAK
doi:10.3906/yer-0809-3 First published online 30 April 2009

Mineral and Whole-rock Geochemistry of the Kestanbol Granitoid (Ezine-Çanakkale) and its Mafic Microgranular Enclaves in Northwestern Anatolia: Evidence of Felsic and Mafic Magma Interaction

SABAH YILMAZ ŞAHİN[1], YÜKSEL ÖRGÜN[2], YILDIRIM GÜNGÖR[3], A. FETİ GÖKER[3], ALİ HAYDAR GÜLTEKİN[2] & ZEKİYE KARACIK[2]

[1] İstanbul University, Engineering Faculty, Department of Geophysical Engineering, Avcılar, TR–34320 İstanbul, Turkey (E-mail: sabahys@istanbul.edu.tr)

[2] İstanbul Technical University (İTÜ), Faculty of Mines, Department of Geological Engineering, Maslak, TR–34469 İstanbul, Turkey

[3] İstanbul University, Engineering Faculty, Department of Geological Engineering, Avcılar, TR–34320 İstanbul, Turkey

Received 04 September 2008; revised typescript receipt 21 April 2009; accepted 24 April 2009

Abstract: The Miocene Kestanbol granitoid, in Ezine-Çanakkale, Turkey, is one of post-collision granitoids of western Anatolia, which have been related to the the late Cretaceous collision between the Anatolide-Tauride platform and the Pontides. Magmatism began during the early Miocene, with coeval alkaline to calc-alkaline plutonism and volcanism, controlled by the regional tectonic evolution. The Kestanbol pluton intruded regionally metamorphosed basement rocks. Volcanic and volcano-clastic sedimentary rocks overlie the pluton, which is bounded in the west and east by major faults. The pluton is frequently cut by felsic and mafic dykes and includes mafic microgranular enclaves (MMEs) that are mixing products of coeval felsic and mafic magmas.

The Kestanbol granitoid is quartz monzonitic but the MMEs include monzonite, monzodiorite, and quartz monzodiorite. There are some special mixing textures such as antirapakivi, blade-shaped biotite, acicular apatite, spongy-cellular plagioclase and spike-zoned plagioclase in MME-host rock pairs. MME and host rock pairs display mineralogical similarities and they indicate some interactions and parallel evolution with each other. However, they have distinct major and trace element behaviour. The mineralogical and petrographical properties of the felsic and mafic dykes resemble the felsic host rocks and MMEs respectively.

The results of the mineral chemistry showed that plagioclases are albite-labradorite (An_{8-50}), amphiboles are magnesio-hornblende and biotites are Mg-biotites in MME-host rock pairs. The amphibole compositions of the Kestanbol granitoid and its MMEs are somewhat similar ($Mg/Mg+Fe^{+2}$ = 0.55–0.87 and 0.55–0.74). The FeO^t/MgO ratio of biotites in these rocks is between 1.01 and 1.55.

These rocks are post-collisional, subalkaline, metaluminous and high-K calc-alkaline, I-type in character, and derived from hybrid magma that originated from the mixing of coeval mafic and felsic magmas in different ratios and at different depths.

Key Words: Kestanbol granitoid, magma mingling/mixing, mafic microgranular enclave (MME), hybrid magma, post-collision

Kestanbol Granitoyidi ve Mafik Mikrogranüler Enklavlarının (Ezine Çanakkale) Mineral ve Tüm –Kayaç Jeokimyası: Felsik ve Mafik Magma Etkileşiminin Kanıtları

Özet: Ezine-Çanakkale civarında yüzeylenen Miyosen yaşlı Kestanbol granitoyidi, Batı Anadolu'da, Anatolid-Torid Platformu'nun geç Kretase'de çarpışmasıyla oluşan, çarpışma sonrası granitoyidlerden bir tanesidir. Erken Miyosen'de başlayan çarpışma sonrası magmatizma, alkalinden-kalkalkaline değişen özelliklerde olup, bölgesel tektonik kontrollü olarak, plütonizma ve volkanizma birlikte eşyaşlı olarak oluşmaktadır. Kestanbol granitoyidi bölgesel metamorfik temel kayaçlar içerisine sokulum yapmış ve volkanik-volkano-klastik sedimanter kayaçlarla örtülmüştür. Buna ilaveten plütonun batı ve doğu kesimleri büyük faylarla sınırlanır. Pluton eşyaşlı mafik ve felsik magmaların karışım ürünleri olan mafik magmatik enklavlar içerir ve sık sık felsik ve mafik dayklarla kesilir.

Kestanbol granitoyidi quvars monzonitik bileşimdedir ancak bu kayaçların enklavları monzonit, monzodiyorit ve kuvars monzodiyorit bileşimdedir. MME-Ana kaya çiftleri, antirapakivi, bıçağımsı biyotit, iğnemsi apatit, süngerimsi-hücremsi plajiyoklaz ve çivi başlarına benzeyen yamalar içeren plajiyoklaz dokusu gibi bazı özel '*mixing*' dokuları içermektedirler. Her iki kayaç grubu da mineralojik benzerliklerin yanısıra birbirleriyle bazı etkileşimler ve benzerlikler sergilemektedir. Buna karşın, majör ve iz element davranışları bakımından farklılıklar sunmaktadırlar. Felsik ve mafik damar kayaçlarının mineralojik-petrografik özellikleri felsik ana kayaçlara ve mafik MME'lara benzerler.

Mineral kimyası sonuçlarına göre plajiyoklazlar albit-labrador (An_{8-50}), amfiboller magnezyo-hornblend ve biyotitler Mg-biyotit bileşimindedirler. Kestanbol granitoyidi amfibol minerallerinin $Mg/Mg+Fe^{+2}$ = 0.55–0.87 değeri, MME'lardaki $Mg/Mg+Fe^{+2}$ = 0.55–0.74 değeri ile benzerdir. Biyotitlerin FeO^{t}/MgO oranı ise, 1.01 ve 1.55 arasındadır.

Bu kayaçlar çarpışma sonrası kökenli, subalkalin, metaluminalı, yüksek K-'lu kalk-alkalin karakterlidir ve eşyaşlı felsik ve mafik magmaların değişik oranda ve değişik magma ortamlarında karışması ile oluşmuşlardır.

Anahtar Sözcükler: Kestanbol granitoyidi, magma mingling/mixing, mafik mikrogranüler anklav (MME), melez magma, çarpışma sonrası

Introduction

Mafic microgranular enclaves play a significant role in the genesis of granitoid rocks, particularly calc-alkaline granitoids. In granitoid systems, among many different types of interaction between coeval felsic and mafic magmas, three main processes are distinguished: mixing, mingling and chemical exchange (Barbarin 1988, 2005; Didier & and Barbarin 1991; Barbarin & Didier 1992).

Magma mixing causes homogenization of the interacting melt phases and the partial dissolution of early crystals (corrosion) in new hybrid magma, whereas, mingling or co-mingling involve partial mixing or interpretation of pervasive changes in felsic-mafic magmas (Barbarin & Didier 1992). Magma mingling products are mafic magmatic enclaves (MME) that are classically considered as globules of quenched mafic magmas within the felsic host magmas (Vernon 1986). Chemical exchange generally forms after thermal equilibration, in which major element diffusion between melts of contrasting composition occurs along contact surfaces of felsic and mafic magmas (Barbarin & Didier 1992).

In western Anatolia, calc-alkaline and I-type granitoid rocks, with different ages and compositions display extensive evidence of interactions between mafic and felsic magmas. The Kestanbol pluton, therefore, must bear some field, petrographic, mineralogical, and geochemical features relevant to such magmatic processes such as magma mixing and magma mingling.

The Kestanbol granitoid intruded crustal metasedimentary rocks. All these post-collisional plutons in western Anatolia are related to the collision between the Anatolide-Tauride platform and the Pontides that occurred during the late Cretaceous period (Figure 1; Karacık & Yılmaz 1998). The N–S convergence continued until the Neogene and magmatism began during the early Miocene (Karacık & Yılmaz 1998). The plutonic products of this magmatism are associated with volcanic and volcano-sedimentary rocks.

This paper presents a comprehensive petrography, mineral chemistry, and whole rock geochemistry of the Kestanbol granitoid and its microgranular enclaves. In addition, the possible origin of the microgranular enclaves and the

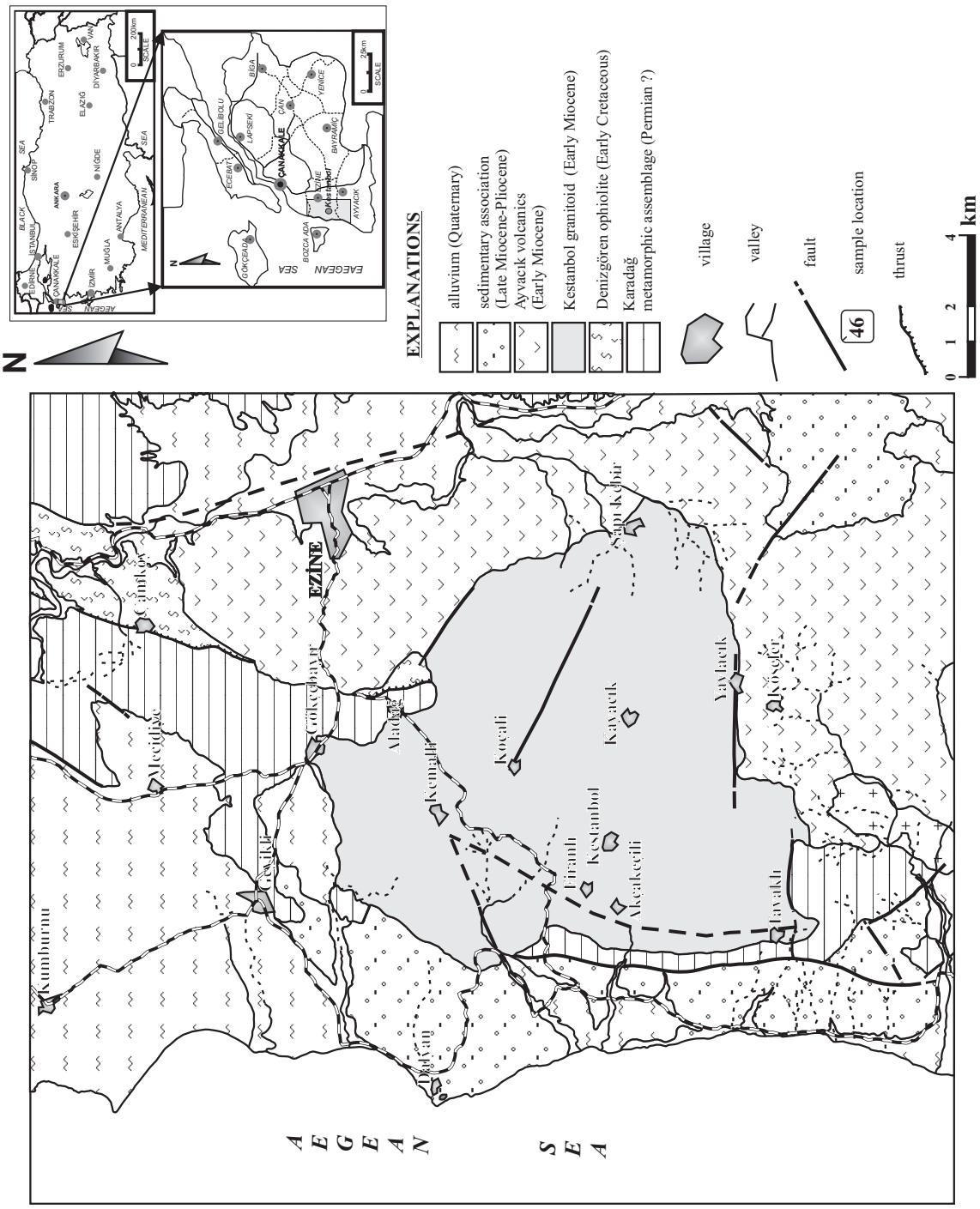

Figure 1. Geological map of the Kestanbol (W Ezine-Çanakkale) area (modified from Karacık & Yılmaz 1998).

interaction processes between acidic and basic magmas in this plutonic environment are discussed.

Geological Setting

Western Anatolia has been characterized by extensive magmatic activity during late Eocene to late Miocene time (Yılmaz 1997; Karacık & Yılmaz 1998; Delaloye & Bingöl 2000; Yılmaz *et al.* 2001; Aldanmaz 2006). This magmatic activity resulted in coeval plutonism and volcanism with alkaline to calc-alkaline features and was controlled by the regional tectonic evolution. Regional tectonic and magmatic activity during most of the Miocene is considered to be largely influenced by lithospheric spreading and thinning subsequent to earlier plate collision and stacking (Aldanmaz 2006). The magmatism started in the Oligocene, intensified during the early Miocene and waned in the late Miocene–Pliocene (Yılmaz 1997). In western Anatolia, two geochemically distinct phases of magmatic activity are distinguished. The early phases that produced the granitic plutons and associated intermediate volcanic rocks were commonly calk-alkaline in composition (Yılmaz 1997). Alkaline rock varieties during this period were rare. The late phase that produced basaltic lavas was generally alkaline or transitional (Yılmaz 1997).

The north and northwestern Anatolia granitoids belong to two large groups according to $^{40}Ar/^{39}Ar$ age determination by Delaloye & Bingöl (2000). The first group is comprised of young granitoids (late Cretaceous to late Miocene) mainly distributed in the western part and the second consists of older granitoids (pre-Ordovician to late Jurassic) concentrated in a belt in northwestern and northern Anatolia. The young granitoids are intrusive into the old granitoid belt. Their geology, petrology, geochronology and geodynamic evolution have been studied (Birkle & Satır 1992; Karacık 1995; Yılmaz 1997; Karacık & Yılmaz 1998; Delaloye & Bingöl 2000; Okay & Satır 2000; Yılmaz *et al.* 2001; Aldanmaz 2006). The Kestanbol granitoid, one of the intrusive bodies in the Western Anatolia magmatic province, is located south of Ezine-Çanakkale. Intrusive rocks can be found along a N–S trend within the major tectonic belt named the Sakarya Continent. The Kestanbol granitoid is a calc-alkaline, post-collisional, and I-type pluton that has a Miocene age (21.28 Ma; Birkle & Satır 1992) within the Sakarya Continent, which is bounded by the Intra Pontide Suture Zone on the north and the İzmir-Ankara Suture Zone on the south. The Sakarya Continent consists of metamorphic and non-metamorphic Palaeozoic rocks overlain by Mesozoic and Cenozoic rocks (Figure 1; Yılmaz 1997).

Geological properties of the Kestanbol granitoid were determined in detail by Karacık & Yılmaz (1998). In the studied area the main geological units include Palaeozoic–Permian metamorphic rocks, Triassic ophiolitic rocks, a Miocene granitoid pluton and sedimentary rocks. The Kestanbol granitoid was emplaced into the regionally metamorphosed basement rocks of the Sakarya Continent and generated a well-developed metamorphic aureole to the west, north and northeast (Andaç 1973; Karacık & Yılmaz 1998). To the south, volcanic and volcanoclastic sedimentary rocks overlie the pluton. In addition, the western and eastern parts of the pluton are bordered major faults (Figure 1). The granitic magma appears to have ascended through the extensional zones, formed where the bends or releasing steps along the NE–SW occurred (Karacık 1995). The Kestanbol pluton consists of monzonitic rocks and was derived from crustal melts that mixed with mantle-derived mafic magma. The pluton includes mafic microgranular enclaves (MME) that are products of mixing of felsic and mafic magmas (Yılmaz Şahin *et al.* 2004; Figure 2). It is cut by leucogranitic and lamprophyric dykes that are commonly found around Aladağ and Firanlı villages (Figure 1).

Petrography

Kestanbol Granitoid (KG)

The Kestanbol granitoid (KG) crops out over an area of 200 km^2 to the south of Ezine (Figure 1), and is emplaced into the regionally metamorphosed basement rocks. The pluton is lithologically made up of monzonitic rocks and crosscut by a set of dykes of aplite, pegmatite, lamprophyre and porphyritic latite. The width of the dykes varies from 1–2 cm to 1–2 m.

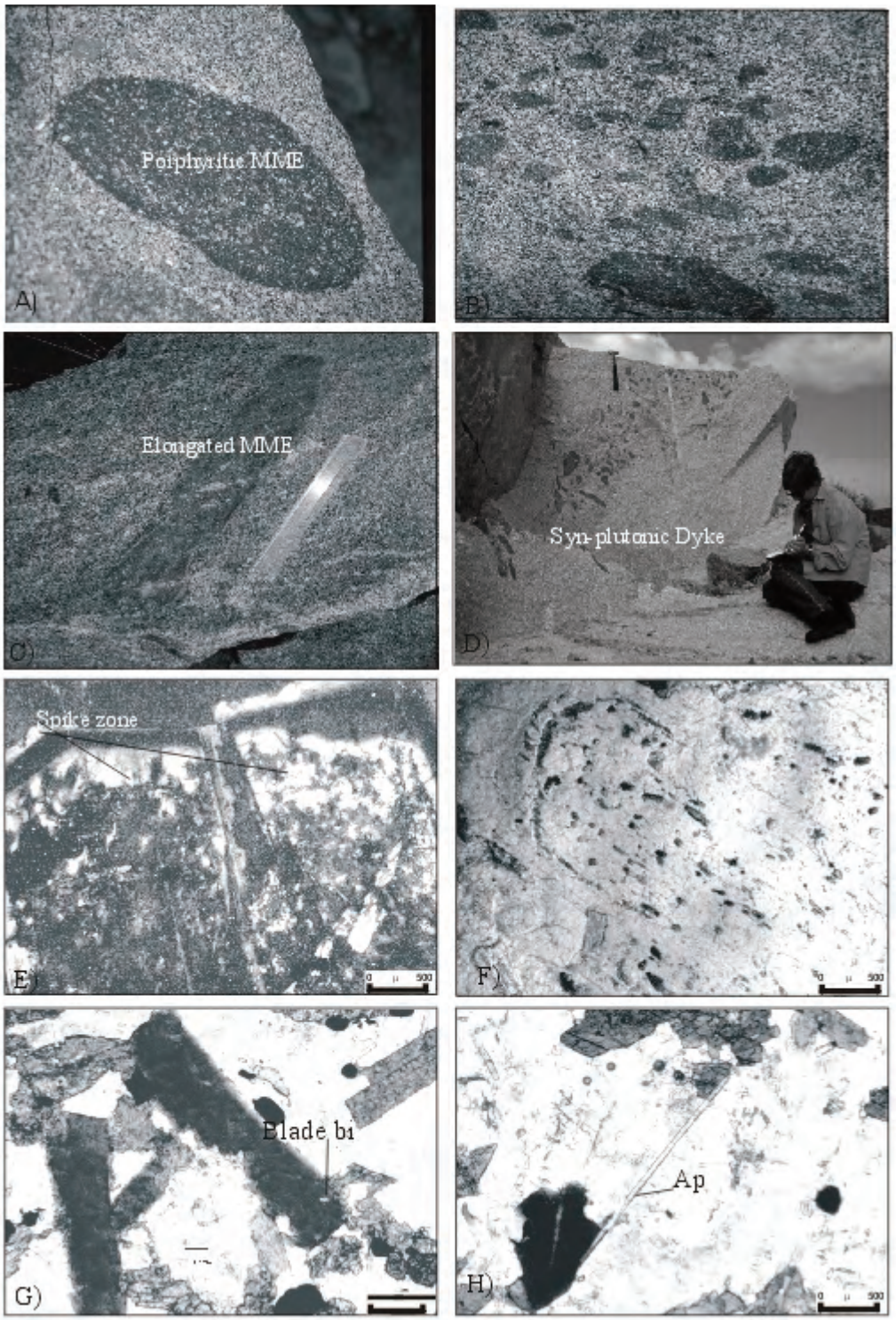

Figure 2. Field photographs showing the mafic microgranular enclaves: **(a)** Sharp-boundary between ellipsoidal-ovoid shaped MME and KG, **(b)** different sizes and shaped enclaves, **(c)** elongated MME, **(d)** syn-plutonic dyke within the Kestanbol pluton. Microscopical pictures of some special mixing texture: **(e)** spike zones in plagioclase, **(f)** biotite/hornblende zone in plagioclase phenocryst, **(g)** blade-shaped biotite, **(h)** acicular apatite within MMEs and their host rocks. plj– plagioclase; bi– biotite; ap– apatite.

The dykes are concentrated around Firanlı and Aladağ villages (Figure 1). Perthitic K-feldspar is the dominant rock-forming mineral in the dykes. Along the east and southeast borders, the plutonic rocks pass gradually into fine-textured porphyritic volcanic rocks, including rhyolite, rhyodacite and dacite, and andesitic and trachyandesitic pyroclastic rocks. The volcanic rocks consist mainly of different proportions of plagioclase, quartz, K-feldspar (sanidine), biotite, hornblende, opaque minerals (magnetite and pyrite) and accessory minerals (titanite, epidote, apatite, zircon). The pluton is bounded by sedimentary rocks along the north and northwest borders.

The Kestanbol granitoid is composed of coarse-grained equigranular quartz monzonite and subordinate monzogranite (Figure 3; Debon & Le Fort 1983), which can sometimes be fine-grained and porphyritic with K-feldspar megacrysts and abundant plagioclase phenocrysts. The porphyritic granitoid includes large (1–5 cm), euhedral, pink megacrysts of orthoclase (wt% 20–75 by volume) set in a medium-coarse grained subhedral-anhedral groundmass consisting of ortoclase (20–75 wt%), plagioclase (An_{20-35}) (10–45 wt%), quartz (12–35 wt%), hornblende (5–15 wt%), biotite (2–10 wt%), rarely pyroxene (2–5 wt%) with accessory minerals (1–2 wt%) such as titanite, apatite, zircon, allanite, epidote and opaque minerals (magnetite, ilmenite, pyrite and rutile). Some radioactive accessory minerals (titanite, apatite, zircon, allanite, epidote, thorite, and uranothorite; 0.1–4.5 wt%) are also common in the pluton (Örgün *et al.* 2007). As the U-Th values are very high in the Kestanbol pluton, the pluton is referred to as radioactive (Andaç 1973; Örgün *et al.* 2007). Zircon was also observed as a part of the magnetite. Around zircon inclusions in hornblende and biotite minerals, radioactive pleochroic aureoles were seen. Secondary minerals are chlorite, sericite, muscovite and iron-oxide minerals.

Mafic Microgranular Enclaves (MMEs)

The mafic microgranular/magmatic enclaves (MME) are particularly abundant in the calc-alkaline Kestanbol granitoid (KG) and provide information on the role of mafic magmas in the initiation and evolution of felsic host magmas (Didier & Barbarin 1991; Yılmaz & Boztuğ 1994). Different types of MME within Kestanbol granitoid have been distinguished by their grain size, texture, structure, mineralogical composition, nature and abundance of phenocrysts, external morphology and contacts with host granitoids (Yılmaz Şahin *et al.* 2004; Figure 2a).

The mafic microgranular enclaves (MMEs) may be of fundamental significance in interpreting the history of the KG. They are disseminated throughout south and southwestern part of the pluton. Their shapes, chemical composition, mineralogy and texture undoubtedly support a magmatic origin as a result of repeated interactions between acid and basic magmas (Barbarin 1988). They are always darker than the host rock, generally rounded or ellipsoidal in shape, and elongated parallel to the flow direction of the felsic host rock due to plastic deformation during the partially liquid state (Vernon *et al.* 1988; Figure 2c). They commonly have sharp contacts with felsic host rock but diffuse contacts were also observed, which can be attributed to the undercooling and mingling of hybrid microgranular enclave globules formed by the mixing of mafic and felsic magmas. The size of the MMEs commonly varies from 1 to 50 cm and sometimes may reach up to 1 m across. They have a holocrystalline-hypidiomorphic inequigranular texture with common plagioclase phenocrysts. The composition of the MMEs varies from monzonite-quartz monzonite to diorite and quartz diorite (Figure 3; Debon & Le Fort 1983). Their mineralogical composition is similar to the monzonitic host rock but differs in modal proportions. The monzonitic rocks consist of plagioclase (An_{18-22}) -hornblende-biotite-K-feldspar (orthoclase) -quartz-pyroxene, together with accessory minerals such as apatite, titanite, epidote, and Fe-Ti oxide minerals. More mafic minerals are seen in the fine-grained margin of the MMEs. Both the KG and its MMEs show some mixing texture such as antirapakivi, lath-shaped small plagioclase within large plagioclase, poikilitic K-feldspar/plagioclase, rarely acicular apatite in host rocks and commonly, spike zone in plagioclase, hornblende/biotite zones in K-feldspar/plagioclase

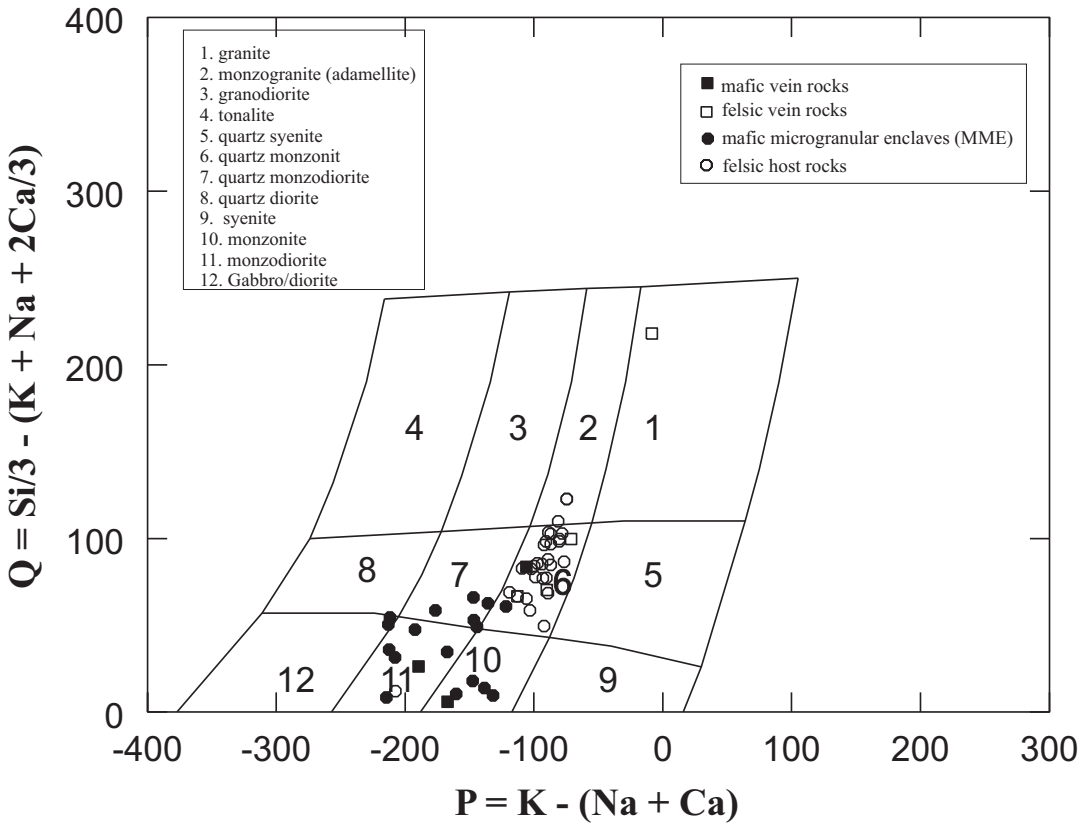

Figure 3. Nomenclature diagram (Debon & Le Fort 1983) of Kestanbol granitoid (KG) and their mafic microgranular enclaves (MMEs).

megacrystals, blade-shaped biotite, acicular apatite, poikilitic K-feldspar/plagioclase, spongy cellular plagioclase and dissolution melting in plagioclase (Hibbard 1991, 1995; Fernandez & Barbarin 1991) in the MMEs (Figure 2e, f, g & h).

K-feldpar megacrysts are found both in the KG and in the MME where they are partially dissolved, or at the enclave-host contact, providing persuasive evidence for the importance of magma mixing (Vernon 1986). These megacrysts compositionally and texturally closely resemble crystals from the host granitoid and are inferred to have been tranferred from the host granitoid while both magmas were still partially molten (Vernon 1986; Barbarin 1990).

Vein Rocks

Around Aladağ, Firanlı and the northwestern Kestanbol villages the Kestanbol pluton is cut by an extensive set of felsic and mafic dykes. Aplitic, pegmatitic and granophyric dykes are fine- to medium-grained, equigranular, and locally porphyritic, where K-feldspar megacrysts are present. They include K-feldspar (generally perthitic), plagioclase, quartz with minor biotite and accessory minerals such as apatite, zircon and opaques. However, the mafic dykes have lamprophyre, leucite porphyry and microdioritic compositions. They are dark, fine-grained, and have a sharp contact with felsic host rocks. All of these dykes were injected after the crystallization of the KG and they generally follow the joint planes. However, there are also several fault zones both in these localities and other parts of the pluton and alteration is common in these regions. Association of vein rocks, faults and hydrothermal alteration in these zones has created high radioactivity concentrations (Örgün *et al.* 2007).

Mineral and Whole Rock Geochemistry

Analytical Methods

A total of 57 samples that were taken from the MME-host rock pairs, host rocks without the MMEs, felsic and mafic vein rocks were subjected to whole rock major and trace element chemical analysis (Tables 1–3) using the ICP-MS of the ACME Laboratory in Canada.

Mineral chemical analyses were made on 16 polished MME-host rock samples. Samples were prepared for electron-microprobe studies at the Geochemistry laboratory, İstanbul Technical University. Carbon-coated thin sections were analysed at the TÜBİTAK Marmara Research Center (MAM-Gebze-İstanbul) Field Emission Scanning Electron Microscope (SEM) Laboratory using the JEOL JSM-6335F-EDS (EDAX) electron-microprobe (Table 4). One thin section only was analysed at the Mineralogy and Petrology Institute, Hamburg University, using a CAMECA SX-100 electron-microprobe (equipped with wavelength an energy dispersive spectrometers) at the following operating conditions: accelerating voltage 15 kV, beam current 20 nA, and beam diameter 5 μm.

Mineral Geochemistry

Plagioclase. Thirty-six analyses of feldspar minerals were obtained in the Kestanbol granitoids and its MMEs (Table 4). Plagioclases are found as phenocrysts within the host rocks, but in the MMEs they form both megacrysts and small crystals within the enclave groundmass. Large plagioclase phenocrysts in the MME have similar shape and composition to those in the monzonitic host rocks. They show variable types of compositional zoning as patchy, normal and rarely reverse zones. Plagioclases, thus, were analysed from at least two points for a single crystal, such as rim and core during the SEM studies (Table 4a, b). These minerals represent a wide range of composition within the Kestanbol granitoids (KG) and their MMEs. The composition of plagioclases ranges from An_{12} (albite) to An_{48} (andesine) in felsic host rocks and from An_{8} (albite) to An_{50} (andesine/labradorite) in the MMEs (Figure 4a). The cores of the pluton and its MMEs are relatively more calcic in contrast to sodic rims. These values are similar to each other due to the chemical interaction between felsic and mafic magmas (Barbarin & Didier 1992; Barbarin 1999).

Plagioclases in the MME and host rocks show some disequilibrium texture such as poikilitic plagioclase, lath-shaped small plagioclase in large plagioclase, spike zones within a plagioclase in the KG and its MMEs (Figure 2b). Especially, disequilibrium textures in plagioclase phenocrysts reflect a magma mixing process in the felsic host and mafic magmas.

Amphibole. The representative amphibole analyses from the KG and their MMEs are given in Table 4c and d. Amphiboles are abundantly found both in felsic host rocks and their MMEs. Amphiboles belong to the calcic group with a dominant chemical composition of magnesio-hornblende (Leake *et al.* 1997; Yavuz 2007) (Figure 4b). The studied amphiboles had high FeO wt% (11.69–24.28 in host rocks and 8.21–16.62 in the MMEs), but low MgO wt.% (10.38–18.10 in felsic host rocks and 11.31–15.47 in the MMEs), with the $Mg/(Mg+Fe^{2+})$ ratios ranging from 0.54 to 0.80. The compositions of amphiboles within the KG and its MMEs were indistinguishable, except that a few amphiboles in the KG were observed to have higher $Mg/(Mg+Fe^{2+})$ ratios with decreasing Si atomic per formula unit (*apfu*) of amphiboles, which probably evolved as a result of the changing silica activity of the binary (mafic-felsic) magma mixing system. On the basis of Al-in hornblende geobarometer and hornblende-plagioclase geothermometer evaluations (Blundy & Holland 1990), the KG was formed under conditions of 1.17–3.6 kbar and 659–799 °C, whereas geothermobarometric calculations for the samples from the MME yielded 1.24–3.84 Kbar and 692–766 °C. It is suggested that mafic-felsic magma mixing and mingling of MME globules within the felsic KG host might have occurred at 3.5 Kbar pressure, equivalent to a shallow crustal level (~12 km depth). These features are similar to these of the Malanjkhand granitoids from central India (Kumar & Rino 2006). The emplacement of the Kestanbol granitoid was closely preceded by the coeval, felsic Ayvacık volcanics, whose geological and geochemical features are similar to the Kestanbol pluton (Karacık & Yılmaz 1998).

Table 1. Results of whole rock major (wt%), trace (ppm) and REE (ppm) chemical analysis of Kestanbol granitoid. tFe_2O_3– total iron; LOI– loss on ignition.

Elements	1	2	3	4	5	6	7	8	9	10	11	12	13	14	15	16	17	18	19	20	21	22	29	32	27	61	*62*
SiO_2	62.99	60.00	61.95	63.18	67.52	62.16	61.81	63.37	64.70	63.97	63.09	64.56	65.35	62.51	61.97	59.88	60.65	64.88	64.26	63.97	62.51	62.31	63.80	63.47	59.99	63.43	*62.20*
TiO_2	0.55	0.68	0.60	0.57	0.42	0.59	0.62	0.54	0.5	0.55	0.56	0.52	0.48	0.62	0.61	0.63	0.61	0.50	0.50	0.53	0.56	0.56	0.53	0.55	0.66	0.56	*0.64*
Al_2O_3	15.83	15.74	15.81	15.63	14.75	15.79	15.78	15.56	15.39	15.58	16.06	15.61	15.50	16.14	16.30	16.24	16.14	15.48	15.59	15.48	15.57	15.58	15.72	15.53	16.65	16.24	*16.21*
tFe_2O_3	4.34	5.64	4.71	4.44	3.26	4.72	4.93	4.30	3.87	4.30	4.26	3.89	3.60	4.63	4.71	4.94	5.10	3.69	3.76	4.31	4.44	4.79	4.20	4.44	4.95	4.31	*4.73*
MnO	0.08	0.10	0.08	0.08	0.07	0.07	0.08	0.07	0.07	0.07	0.07	0.07	0.07	0.09	0.09	0.08	0.1	0.08	0.07	0.08	0.08	0.10	0.07	0.07	0.10	0.08	*0.09*
MgO	2.12	2.55	2.25	2.12	1.41	2.26	2.44	2.12	1.90	1.98	2.21	2.11	1.99	2.25	2.29	2.36	2.48	1.94	2.11	2.01	2.70	2.16	1.89	2.09	2.41	2.15	*2.39*
CaO	4.22	5.21	4.35	4.14	3.09	4.32	4.39	3.65	3.61	4.00	4.09	3.62	3.5	4.49	4.53	4.81	5.02	3.56	3.79	4.01	4.09	4.73	3.83	3.94	4.50	4.09	*4.47*
Na_2O	3.65	3.45	3.64	3.56	3.63	3.6	3.62	3.61	3.6	3.38	3.67	3.50	3.56	3.61	3.65	3.71	3.53	3.71	3.54	3.59	3.37	3.38	3.57	3.66	3.76	3.81	*3.72*
K_2O	4.51	4.76	4.99	4.79	4.61	4.72	4.53	4.95	4.72	4.71	4.60	4.68	4.53	4.45	4.21	4.07	4.59	4.45	4.46	4.48	4.29	4.85	4.54	4.67	5.50	4.53	*4.42*
P_2O_5	0.28	0.42	0.34	0.30	0.21	0.33	0.33	0.31	0.26	0.24	0.28	0.23	0.20	0.27	0.31	0.32	0.36	0.22	0.23	0.25	0.27	0.34	0.24	0.31	0.41	0.28	*0.31*
LOI	1.00	1.00	0.80	0.70	0.60	0.90	1.00	1.00	0.90	0.80	0.60	0.80	0.80	0.50	0.90	2.50	0.90	1.00	1.30	0.90	1.70	0.70	1.10	0.80	0.60	0.30	*0.60*
A/CNK	0.85	0.77	0.82	0.84	0.89	0.83	0.84	0.87	0.87	0.87	0.87	0.90	0.90	0.85	0.87	0.84	0.81	0.89	0.89	0.86	0.88	0.80	0.88	0.85	0.82	0.87	*0.85*
TOTAL	99.57	99.55	99.52	99.51	99.57	99.46	99.53	99.48	99.52	99.58	99.49	99.58	99.59	99.56	99.57	99.54	99.48	99.51	99.61	99.61	99.58	99.50	99.48	99.53	99.54	99.78	*99.79*
V	103	132	108	95	66	99	108	94	82	88	88	79	70	103	92	104	111	69	73	86	87	96	81	83	120	94	*97*
Co	13	16	14	13	10	14	14	13	12	12	13	12	11	13	13	14	14	11	11	12	13	12	11	12	15	11	*12*
Ga	19	19	19	19	18	18	18	19	18	17	18	18	18	18	19	19	20	19	19	18	18	17	17	17	18	18	*17*
Cu	10	12	10	12	6	45	20	16	6	17	15	7	7	23	9	27	16	12	5	10	35	12	4	14	56	55	*09*
Pb	15	13	10	11	22	21	17	20	11	11	28	25	16	11	6	10	11	21	10	12	26	12	9	29	15	07	*10*
Zn	26	21	22	25	24	22	27	19	17	18	27	31	29	28	28	27	32	37	28	22	27	26	22	25	21	62	*20*
Rb	184	176	199	204	256	204	188	204	206	174	178	212	212	174	170	154	165	193	197	203	185	172	186	205	207	180	*180*
Ba	1103	1334	1373	1072	803	1008	1242	1144	1051	1056	1122	1005	913	1101	1054	1159	1348	914	959	1025	1076	1119	960	973	1707	1318	*1220*
Sr	799	1048	955	850	644	861	956	809	836	762	772	650	608	890	899	984	1018	614	649	746	646	894	767	797	1120	860	*891*
Nb	16.7	18.3	22.7	20	19.1	19	19.2	20.4	22.1	20.9	14.7	14.9	14.7	18.5	17.5	17.1	16.1	15.8	15.7	15.1	13.4	17.5	17.2	18	21	16	*21*
Zr	220	237	231	228	184	223	230	244	200	212	200	212	178	212	271	256	264	198	205	211	195	227	197	207	283	246	*206*
Y	24	30	27	25	20	24	26	26	25	27	21	23	21	29	25	25	28	22	23	23	20	26	22	23	30	22	*28*
Hf	6.9	6.9	8.0	7.2	6.8	7.4	7.4	7.8	6.6	7.4	6.5	6.7	6.2	6.6	8.1	8.2	7.9	6.2	6.9	6.9	5.8	7.0	6.5	6.3	8.3	8.1	*7.4*
Th	50	54	62	80	59	62	61	62	59	62	47	58	42	53	47	47	40	43	65	54	36	47	59	65	50	40	*63*
U	11.9	8.2	8..3	17.4	16.1	14.3	15.7	16.3	15.9	14	10.7	11.8	10.4	12.6	17	9.7	9.6	7.5	12.3	14.1	7.3	11.1	15.4	14.3	9.7	9.9	*10.8*
La	78	89	85	91	73	86	90	84	80	80	70	67	71	78	81	84	85	61	81	73	63	84	74	78	82	62	*70*
Ce	139	162	159	159	122	155	162	151	144	147	124	118	122	143	146	147	155	111	140	127	112	148	127	139	178	129	*154*
Pr	15	18	17	17	13	16	18	16	16	13	13	13	16	16	16	17	12	15	14	12	16	16	13	15	19	14	*17*
Nd	51	66	60	60	45	58	63	59	58	55	47	45	46	60	57	56	61	45	50	50	45	59	49	56	77	51	*64*
Sm	9	12	11	10	8	10	11	10	10	9	8	8	7	10	9	9	11	8	8	8	8	10	9	8	12	8.4	*9.9*
Eu	1.84	2.61	2.19	2.07	1.51	2.02	2.24	2.1	1.9	1.83	1.62	1.54	1.53	2.09	2.02	1.99	2.3	1.44	1.54	1.66	1.62	2.18	1.65	1.84	2.42	1.61	*1.65*
Gd	5.59	7.93	6.56	6.51	4.51	5.9	6.72	6.16	6.02	5.62	5.29	4.87	4.93	6.98	6.02	5.81	7.16	5.12	4.98	5.19	4.95	6.79	5.14	5.82	8.16	5.38	*6.85*
Tb	0.83	1.12	1.01	0.94	0.72	0.88	0.99	0.92	0.9	0.93	0.76	0.74	0.73	1.01	0.85	0.82	1.04	0.76	0.79	0.76	0.71	0.94	0.78	0.86	1.20	0.83	*1.10*
Dy	4.12	5.42	4.92	4.51	3.53	4.19	4.52	4.25	4.13	4.48	3.79	3.64	3.65	5.10	4.38	4.41	5.28	3.94	3.83	3.85	3.59	4.89	3.96	4.23	5.77	3.98	*4.76*
Ho	0.73	0.88	0.78	0.74	0.56	0.69	0.76	0.72	0.74	0.81	0.68	0.67	0.64	0.87	0.79	0.77	0.85	0.67	0.73	0.69	0.63	0.81	0.69	0.72	0.86	0.69	*0.80*
Er	2.13	2.47	2.35	2.11	1.77	2.08	2.14	2.17	2.26	2.38	1.80	2.00	1.88	2.54	2.10	2.19	2.33	1.98	1.99	2.04	1.85	2.25	1.95	2.11	2.58	2.00	*2.55*
Tm	0.32	0.36	0.36	0.34	0.29	0.31	0.32	0.34	0.33	0.36	0.27	0.31	0.27	0.38	0.34	0.33	0.35	0.33	0.31	0.31	0.28	0.33	0.33	0.31	0.31	0.28	*0.33*
Yb	2.09	2.35	2.32	2.08	1.81	1.90	2.05	2.12	2.05	2.23	1.80	1.93	1.77	2.34	2.05	2.23	1.95	1.80	1.98	1.84	1.77	1.86	2.02	1.85	2.17	1.82	*2.16*
Lu	0.34	0.35	0.35	0.31	0.25	0.32	0.30	0.33	0.33	0.38	0.29	0.32	0.30	0.34	0.32	0.34	0.33	0.31	0.31	0.31	0.26	0.32	0.32	0.30	0.31	0.26	*0.32*
Eu_N/Eu^*	*0.79*	*0.82*	*0.79*	*0.78*	*0.77*	*0.80*	*0.80*	*0.82*	*0.75*	*0.79*	*0.76*	*0.75*	*0.80*	*0.76*	*0.84*	*0.84*	*0.79*	*0.69*	*0.75*	*0.79*	*0.79*	*0.81*	*0.74*	*0.82*	*0.75*	*0.73*	*0.61*

Fe_2O_3,, total iron , LOI, loss on ignition

Table 2. Results of whole rock major (wt%), trace (ppm) and REE (ppm) chemical analysis of mafic microgranular enclaves of the Kestanbol granitoid.

	1/1	**2/1**	**4/1**	**7/1**	**9/1**	**10/1**	**11/1**	**13/1**	**14/1**	**15/1**	**16/1**	**17/1**	**18/1**	**19/1**	**20/1**	**21/1**	**22/1**	***62/1***
SiO_2	57.97	53.46	56.05	52.34	56.44	58.34	59.19	53.40	52.51	53.73	55.54	51.76	56.70	57.05	57.68	57.65	54.39	*54.38*
TiO_2	0.78	0.97	0.81	1.00	0.84	0.81	0.73	1.01	1.00	0.74	0.78	1.02	0.78	0.79	0.82	0.81	0.90	*0.94*
Al_2O_3	17.11	16.89	17.52	15.19	16.20	16.48	16.92	18.91	17.55	14.49	14.82	16.45	17.08	15.62	17.78	16.51	15.74	*17.62*
tFe_2O_3	6.31	7.75	6.26	7.53	7.02	6.31	5.44	8.43	8.56	7.25	6.85	9.16	6.67	5.91	6.66	6.63	7.51	*7.25*
MnO	0.10	0.14	0.11	0.17	0.12	0.12	0.09	0.10	0.14	0.20	0.15	0.16	0.15	0.16	0.08	0.10	0.16	*0.13*
MgO	3.07	3.93	3.15	5.52	3.76	3.36	2.95	3.25	4.22	7.57	5.50	4.25	3.29	5.02	2.80	3.39	4.47	*4.04*
CaO	4.99	7.03	5.92	7.80	6.02	5.53	4.84	5.06	7.15	7.48	7.35	7.87	5.49	6.16	4.63	5.36	7.27	*6.48*
Na_2O	4.14	3.29	4.10	2.80	4.60	3.72	3.80	4.99	4.25	3.23	3.63	4.02	5.08	3.54	4.65	3.62	3.65	*3.99*
K_2O	3.57	4.38	4.26	4.60	2.01	3.38	4.11	2.05	2.69	3.31	2.64	2.61	2.33	3.76	2.65	3.61	4.10	*3.53*
P_2O_5	0.45	0.67	0.43	0.63	0.67	0.38	0.39	0.68	0.61	0.22	0.26	0.89	0.42	0.32	0.46	0.46	0.67	*0.51*
LOI	1.00	1.10	1.00	1.80	1.80	1.20	1.10	1.80	1.00	1.50	2.20	1.50	1.70	1.30	1.40	1.50	0.80	*0.90*
A/CNK	0.87	0.74	0.79	0.64	0.78	0.83	0.87	0.96	0.77	0.64	0.67	0.69	0.82	0.74	0.94	0.84	0.66	*0.79*
TOTAL	99.63	99.70	99.72	99.65	99.79	99.77	99.69	99.80	99.81	99.86	99.84	99.79	99.83	99.79	99.77	99.74	99.76	*99.79*
V	165	203	155	206	146	151	128	198	216	149	168	250	151	127	157	169	206	*163*
Co	21	25	19	30	23	20	17	24	25	29	25	25	18	22	21	18	24	*23*
Ga	23	20	20	20	23	22	21	30	22	17	17	21	24	22	25	22	19	*20*
Cu	35	80	205	136	28	60	43	45	53	157	91	18	15	13	16	84	09	*95*
Pb	12	12	14	22	10	14	58	34	09	08	13	12	33	10	09	22	10	*29*
Zn	45	35	32	53	34	43	46	87	51	43	34	53	67	47	40	26	37	*39*
Rb	204	237	215	262	123	177	182	201	159	175	109	125	179	213	158	170	154	*200*
Ba	1175	1241	1135	1655	554	1250	1506	786	519	565	606	549	714	1239	963	1361	986	*1046*
Sr	652	1047	796	836	747	657	906	630	784	527	685	815	585	591	834	811	841	*824*
Nb	15	17	16	17	23	14	13	17	17	13	15	21	14	12	13	15	17	*14*
Zr	221	292	200	298	295	238	223	353	327	162	173	315	257	202	256	167	278	*188*
Y	24	32	23	35	21	20	24	25	32	23	26	43	26	20	18	25	39	*19*
Hf	7.3	8.6	6.0	9.0	9.6	7.4	6.9	10.6	9.7	4.7	5.2	9.1	7.2	5.9	6.8	4.9	7.7	*5.5*
Th	27	34	28	31	21	44	33	30	38	29	21	34	27	13	19	27	37	*19*
U	08	08	11	09	22	15	06	10	09	37	05	08	11	08	07	07	07	*6.5*
La	67.1	93.5	67.5	82.8	124.3	80.3	72	109.3	92.6	39.8	40.5	124.3	66.3	45.0	65.6	71.7	106.8	*69.4*
Ce	129.8	187.1	135.1	172.8	202.2	131.7	143.1	196	180.9	80	82.3	256.7	133.6	87.7	122.9	146.1	221.2	*133.6*
Pr	14.16	20.92	14.94	20.40	18.32	12.94	15.11	19.06	19.29	8.83	9.36	28.56	14.89	9.67	12.27	15.93	24.31	*13.30*
Nd	53.7	77.7	55.8	76.6	63.3	45.7	55.4	64.9	71.3	34.4	36.6	105.5	55.3	38	43.8	58.0	90.3	*50.0*
Sm	9.2	13.5	9.4	14.1	10.1	8.5	9.4	10.3	12.6	6.6	6.7	18.5	10.0	7.1	6.7	9.2	16.1	*8.1*
Eu	1.62	2.51	2.00	2.72	1.70	1.24	1.89	1.88	1.52	1.07	1.24	3.03	1.63	1.43	1.55	1.96	2.67	*1.39*
Gd	5.99	9.05	6.09	9.24	5.66	5.41	5.78	6.11	8.09	4.61	4.81	12.19	6.34	4.77	4.14	6.23	10.58	*5.72*
Tb	0.79	1.26	0.80	1.21	0.82	0.69	0.85	0.86	1.10	0.66	0.74	1.68	0.91	0.67	0.56	0.86	1.47	*0.85*
Dy	4.07	5.68	4.08	5.96	3.58	3.60	4.19	4.28	5.35	3.59	4.16	7.93	4.52	3.72	2.68	4.28	6.95	*3.54*
Ho	0.68	0.95	0.69	1.01	0.62	0.63	0.75	0.77	0.96	0.71	0.76	1.36	0.79	0.63	0.53	0.77	1.16	*0.55*
Er	2.08	2.52	1.96	2.88	1.73	1.87	2.18	2.24	2.85	2.12	2.28	3.44	2.21	1.72	1.45	2.05	2.81	*1.80*
Tm	0.29	0.41	0.28	0.39	0.26	0.25	0.31	0.34	0.43	0.31	0.38	0.47	0.31	0.25	0.23	0.28	0.40	*0.26*
Yb	1.77	2.26	1.69	2.37	1.64	1.60	1.89	1.97	2.27	1.86	2.17	2.93	1.93	1.58	1.56	1.78	2.57	*1.58*
Lu	0.30	0.36	0.29	0.37	0.32	0.28	0.30	0.35	0.40	0.29	0.35	0.43	0.31	0.26	0.28	0.29	0.38	*0.26*
Eu_N/Eu*	*0.67*	*0.69*	*0.81*	*0.73*	*0.69*	*0.56*	*0.78*	*0.72*	*0.46*	*0.59*	*0.67*	*0.62*	*0.63*	*0.75*	*0.90*	*0.79*	*0.63*	*0.62*

Fe_2O_3, total iron , LOI, loss on ignition.

Table 3. The results of whole-rock major (wt%), trace (ppm) and REE (ppm) chemical analysis of felsic and mafic dykes of Kestanbol granitoid.

	FELSIC DYKES						MAFIC DYKES					
	26	**32/1**	**42**	**52/1**	**52/2**	**57**	**61/1**	**51/1**	**38/1**	**38/3**	**48**	**67**
SiO_2	64.03	77.71	63.00	40.64	60.40	61.44	54.55	52.70	45.22	52.63	52.81	51.41
TiO_2	0.46	0.09	0.58	0.20	0.38	0.58	0.97	0.73	0.22	0.70	0.83	0.83
Al_2O_3	15.44	11.98	15.84	9.92	17.34	15.29	17.54	18.38	9.11	12.35	15.77	17.27
tFe_2O_3	3.83	0.75	4.11	4.59	1.99	4.42	7.63	6.05	2.96	7.83	7.51	7.20
MnO	0.07	0.01	0.02	0.26	0.07	0.08	0.13	0.13	0.05	0.15	0.13	0.14
MgO	1.78	0.10	2.40	4.45	0.35	2.65	4.09	3.13	10.54	11.48	3.68	3.80
CaO	3.48	0.63	3.47	27.25	2.06	4.79	6.45	6.00	29.3	6.12	8.44	7.16
Na_2O	3.46	3.14	4.53	1.05	3.07	3.38	4.25	3.99	0.08	2.05	3.15	3.54
K_2O	4.83	4.91	4.49	2.11	10.28	4.92	2.95	6.42	0.18	3.27	4.01	5.81
P_2O_5	0.22	0.01	0.28	0.01	0.08	0.30	0.52	0.53	0.05	0.39	0.67	0.67
LOI	1.80	0.70	1.00	9.40	3.70	1.90	0.70	1.40	7.3	2.70	2.60	1.70
A/CNK	0.75	0.49	0.83	0.73	0.64	0.65	0.53	0.79	0.84	0.73	0.83	0.89
TOTAL	**99.40**	**100.03**	**99.72**	**99.88**	**96.02**	**97.85**	**99.78**	**99.46**	**97.71**	**99.67**	**99.61**	**99.53**
V	68	08	89	40	42	94	183	131	34	170	165	178
Co	11	0.80	11	03	1.90	15	22	16	125	38	22	22
Ga	18	16.4	18	13	16	17	22	18	12	17	19	20
Cu	17	19	1.60	101	194	60	59	66	06	22	58	117
Pb	51	17	7.3	65	98	20	11	81	12	43	09	74
Zn	43	05	09	671	334	43	42	38	07	78	40	36
Rb	200	299	165	134	510	211	206	238	9.20	166	102	221
Ba	1148	81	1089	235	1298	1357	1003	1687	46	941	1538	1957
Sr	792	55	607	198	767	890	644	1284	164	760	1252	1588
Nb	17	21	14	13	42	18	14	38	07	21	21	30
Zr	238	104	203	403	274	281	276	544	63.2	246	364	444
Y	23	08	21	21	18	26	26	28	07	34	31	35
Hf	7.3	6.1	6.6	1.2	3.5	1.6	0.7	2.6	1.3	7.5	10.4	11
Th	52	39	40	90.4	142	60.5	35.6	92.1	7.70	9.3	62	85.7
U	10.4	19.9	7.5	31	29	14.5	10.4	31.6	4.70	46.3	18.3	24.2
La	96.1	34.2	68.7	33.7	65	77.00	65.7	99.6	22.2	75	99.5	113
Ce	160.6	46.6	119.3	58.2	127	161.2	134.6	205.2	46.2	154.5	189.8	237
Pr	16.46	4.04	13.11	6.52	13.08	16.77	15.01	21.08	5.95	17.21	22.18	24.93
Nd	58.8	10.7	48.9	26.7	47.6	64.3	62.3	78.2	22.4	65	84.3	88.50
Sm	9.2	1.5	8.1	4.6	7.00	10.7	9.90	12.8	3.40	12	15	14.90
Eu	1.78	0.19	1.75	0.96	1.20	1.80	1.39	2.62	0.72	2.35	3.22	3.36
Gd	5.76	0.92	5.19	3.47	4.71	6.66	6.61	8.09	2.03	8.03	9.35	9.02
Tb	0.82	0.19	0.76	0.52	0.75	1.02	1.07	1.25	0.28	1.21	1.36	1.39
Dy	3.93	1.01	3.60	2.75	3.30	4.86	4.78	5.71	1.19	6.05	6.33	6.28
Ho	0.74	0.20	0.66	0.49	0.49	0.77	0.71	0.93	0.17	1.02	1.06	1.03
Er	2.07	0.74	1.89	1.63	1.38	2.32	2.20	2.47	0.53	2.69	2.89	2.64
Tm	0.32	0.15	0.29	0.24	0.21	0.32	0.28	0.35	0.08	0.41	0.43	0.38
Yb	1.86	1.10	1.77	2.05	1.41	2.00	1.80	2.35	0.44	2.61	2.53	2.50
Lu	0.29	0.19	0.27	0.34	0.23	0.28	0.30	0.37	0.06	0.4	0.37	0.37
Eu_N/Eu^*	0.75	0.49	0.83	0.73	0.64	0.65	0.53	0.79	0.84	0.73	0.83	0.89

Fe_2O_3, total iron , LOI, loss on ignition

Table 4. Representative analyses of **(a)** plagioclases in the Kestanbol pluton, **(b)** plagioclases in mafic microgranular enclaves **(c)** hornblende minerals in the Kestanbol granitoid, **(d)** hornblende minerals in mafic microgranular enclaves **(e)** biotite minerals in the Kestanbol granitoid, **(f)** biotite minerals in mafic microgranular enclaves.

a. Plagioclase - Host

Sample No	*1*		*1**		*1* (Orthoclase)*		*2*	*3*		*6*		*7*	*8*	*9*	*10*	*11*	*12*		*13*	*17*
Comments	Core	Rim	Core	Rim	Core	Rim	Plj.	Core	Rim	Core	Rim	Plj.	Plj.	Plj.	Plj	Plj.	Core	Rim	Plj.	Plj.
SiO_2	62.08	59.96	58.61	63.17	64.41	64.24	61.95	64.63	60.02	65.66	65.87	58.55	62.44	59.35	62.22	61.65	60.48	63.81	63.16	62.09
Al_2O_3	16.26	21.56	25.07	22.29	18.53	18.27	23.75	22.45	23.48	22.47	22.18	23.99	22.51	25.06	23.12	22.58	25.70	23.91	21.45	23.18
CaO	10.85	6.55	7.11	3.80	0.12	0.07	6.97	7.07	7.10	5.63	7.15	6.80	6.82	7.08	5.88	4.91	7.92	6.37	4.05	6.67
Na_2O	10.19	8.29	7.19	9.02	2.39	2.13	6.30	5.63	6.89	6.25	5.70	8.16	6.94	4.91	5.76	8.23	5.98	6.10	5.23	7.10
K_2O	0.57	0.19	0.31	0.41	12.13	12.52	1.04	0.66	-	-	0.52	0.53	-	0.73	1.02	-	0.53	0.53	4.61	0.35
Total	99.95	96.55	98.29	98.69	97.58	97.23	100.01	100.44	97.49	100.01	101.42	98.03	98.71	97.13	98.00	97.37	100.61	100.72	98.50	99.39

* Microprobe analyses

b. Plagioclase - MME

Sample No	*1**			*3*		*6*		*7*	*8*	*9*	*10*	*11*	*12*		*13*	*17*
Comments	Core	Rim	Ortoc.	Core	Rim	Core	Rim	Pl-1	P-1				Core	Rim		
SiO_2	59.19	66.65	64.57	60.18	62.94	61.82	60.25	61.51	60.44	64.27	61.47	65.56	60.84	61.28	62.14	61.68
Al_2O_3	24.87	20.20	18.55	23.59	22.17	23.38	24.95	24.06	25.28	19.41	24.25	23.02	24.73	24.61	23.81	24.05
CaO	6.88	1.20	0.09	5.61	1.36	5.16	6.79	7.39	9.54	1.71	6.90	6.34	6.27	3.13	5.61	6.83
Na_2O	7.21	9.82	2.19	4.22	2.98	7.02	5.48	7.04	4.93	3.15	5.76	6.51	5.19	1.68	7.43	6.05
K_2O	0.38	0.25	12.41	3.77	8.21	0.53	0.71	0.81	0.45	10.45	0.51		0.36	6.39		
Total	98.53	98.12	97.81	97.37	97.66	97.91	98.18	100.81	100.64	98.99	98.89	101.43	97.39	97.09	98.99	98.61

* Microprobe analyses

c. Hornblend-Host

Sample No	*1**				*1*	*2*	*3*	*6*	*7*	*8*	*9*	*10*	*11*	*12*	*13*	*17*
Comment	Core	Rim	Core	Rim												
SiO_2	48.29	48.37	49.01	49.76	40.82	55.75	45.45	49.25	50.36	37.10	48.03	40.01	49.99	48.41	51.63	47.96
TiO_2	0.85	0.84	0.97	0.70	3.93	-	1.55	1.53	-	0.73	-	4.22	-	1.49	-	4.80
Al_2O_3	5.27	4.99	4.71	4.34	11.80	2.85	7.99	6.95	6.13	17.74	6.69	12.77	6.61	7.27	5.58	6.97
FeO	13.26	12.97	12.67	11.85	16.07	11.69	12.72	12.03	12.19	24.28	15.36	18.76	17.90	14.91	13.64	12.48
MnO	0.57	0.46	0.60	0.55	-	-	-	-	-	0.70	-	-	-	-	-	-
MgO	15.17	15.33	15.53	16.19	13.39	15.62	14.86	13.68	14.70	18.10	13.00	12.90	14.92	12.16	14.38	10.38
CaO	11.71	11.88	11.87	11.80	1.24	13.08	12.07	10.51	12.00		12.14		11.02	11.33	11.92	13.54
Na_2O	1.22	1.16	1.23	1.09	-	-	-	-	1.59	-	1.55	0.49	-	1.56	1.42	1.61
K_2O	0.47	0.47	0.43	0.40	9.19		1.16	0.84		0.77	0.91	9.91		1.01		0.76
Total	96.8	96.5	97.02	96.68	96.44	98.99	95.8	96.36	96.97	99.42	99.09	99.06	100.44	98.14	98.57	98.50

* Microprobe analyses

Table 4. Continued.

d. Hornblend - MME

Sample No	***1/1****		***1/1***	***2/1***	***3/1***	***6/1***	***7/1***	***8/1***	***9/1***	***10/1***	***11/1***	***12/1***	***13/1***	***17/1***
Comments	Core	Rim												
SiO_2	49.01	48.76	49.89	56.10	45.92	49.92	53.53	50.03	47.84	48.10	51.40	48.25	52.06	48.33
TiO_2	0.85	0.78	1.90		2.45	1.01		0.82	1.45	1.55		1.13	0.92	1.32
Al_2O_3	4.84	5.42	6.49	7.27	10.93	5.00	2.19	7.72	7.55	6.40	4.53	8.35	4.96	7.50
FeO	12.56	13.39	12.86	8.45	14.09	14.14	8.21	14.11	15.09	14.80	14.90	16.62	12.34	15.98
MnO	0.58	0.61	-	-	-	-	-	-	-	-	-	-	-	0.94
MgO	15.47	15.14	13.32	13.19	13.24	13.37	13.95	12.72	12.75	1.49	15.05	11.76	14.61	11.31
CaO	11.84	11.71	10.24	11.25	6.30	12.52	19.87	12.26	13.17	12.95	13.10	11.46	11.65	11.40
Na_2O	1.14	1.30	1.57	2.34	-	-	-	-	-	1.49	-	-	1.79	1.66
K_2O	0.53	0.51	-	-	-	0.43	-	-	-	0.64	0.75	1.42	-	1.00
Total	96.82	97.62	96.27	98.60	97.22	96.39	97.75	97.66	97.85	98.89	99.73	98.99	98.33	99.40

* Microprobe analyses

e. Biotite - Host

Sample No	***1****		***1***	***2***	***3***	***6***	***7***	***8***	***9***	***10***	***11***	***12***	***13***	***17***
Comments	Core	Rim												
SiO_2	36.82	37.04	36.78	39.00	38.25	40.65	40.16	38.27	37.59	39.41	39.24	39.61	40.41	40.13
TiO_2	4.35	4.00	2.88	4.86	5.35	4.10	4.23	4.25	3.80	3.97	4.16	3.92	4.96	4.87
Al_2O_3	13.54	13.18	12.20	13.28	13.30	12.05	13.34	15.15	14.44	13.18	14.60	14.32	13.45	13.41
FeO	16.34	16.52	15.87	13.78	17.28	16.72	16.35	17.13	18.37	17.37	18.77	18.27	16.93	18.05
MnO	0.32	0.33	0.77	-	-	-	-	0.60	-	-	-	0.44	-	-
MgO	14.31	14.66	14.14	16.04	13.42	13.80	14.00	15.25	13.52	13.09	13.75	13.29	13.16	13.14
Na_2O	0.12	0.09	1.14	0.63	1.04	-	-	-	-	1.81	-	-	0.98	-
K_2O	8.58	8.44	7.76	10.00	9.24	9.87	10.31	8.82	10.72	8.62	10.10	10.47	9.91	9.91
Total	94.39	94.27	94.47	97.59	97.88	97.19	98.39	99.47	98.44	97.45	100.62	100.32	99.80	99.50

* Microprobe analyses

f. Biotite - MME

Sample No	***1****		***1***	***2***	***3***	***6***	***7***	***8***	***9***	***10***	***11***	***12***	***13***	***17***
SiO_2	36.85	36.42	40.42	38.72	40.86	38.66	38.94	36.44	38.78	40.32	39.07	40.08	40.18	38.58
TiO_2	4.66	4.38	4.65	5.05	5.32	4.40	5.42	2.65	3.49	4.02	3.95	3.41	4.14	4.73
Al_2O_3	13.32	13.55	13.79	14.31	14.05	12.24	12.88	13.37	12.26	12.89	13.35	14.62	13.19	13.36
FeO	16.62	16.45	15.98	15.33	17.18	15.84	16.60	19.11	18.18	19.13	18.19	19.31	17.23	18.29
MnO	0.33	0.32	-	-	-	-	-	0.40	-	-	0.52	-	-	-
MgO	14.19	14.19	15.32	15.16	14.15	13.44	13.99	13.24	12.66	13.75	14.28	12.46	13.34	12.92
CaO	0.05	0.04		2.04	-	1.20	1.87	0.70	2.60	-	-	-	-	-
Na_2O	0.12	0.12	-	-	-	-	-	-	-	-	-	-	-	-
K_2O	0.12	7.81	9.73	9.40	10.24	9.18	10.29	9.00	9.66	9.88	10.38	8.91	10.04	10.23
Total	86.14	93.28	99.89	100.01	101.8	94.96	99.99	94.91	97.63	99.99	99.74	98.79	99.01	98.11

* Microprobe analyses

Biotite. A total of 28 point analyses of biotite from the KG and the MMEs are given in Table 4e and f. Biotite analyses from the KG and the MMEs were recalculated using the Mica+ software (Yavuz 2003a). Biotite is the most abundant ferromagnesian mineral in the KG and its MMEs. Compositionally, biotite displays a limited range for the mole fraction of iron [X_{Fe} = (Fe+Al^{VI})/(Fe+Mg+Al^{VI})] ranging from 0.32 to 0.45 in the quartz monzonite, but the variation of X_{Fe} in MME is between 0.36 and 0.50. In terms of Mg – (Al^{VI}+Fe^{3+}+Ti) – (Fe^{2+}+Mn) ternary components (Foster 1960; Yavuz 2003b), the compositions of biotite from the KG and the MMEs belong to the Mg-biotites (Figure 5a). The FeO_{tot}/MgO ratios of biotites in the KG and the MMEs range from 0.86 to

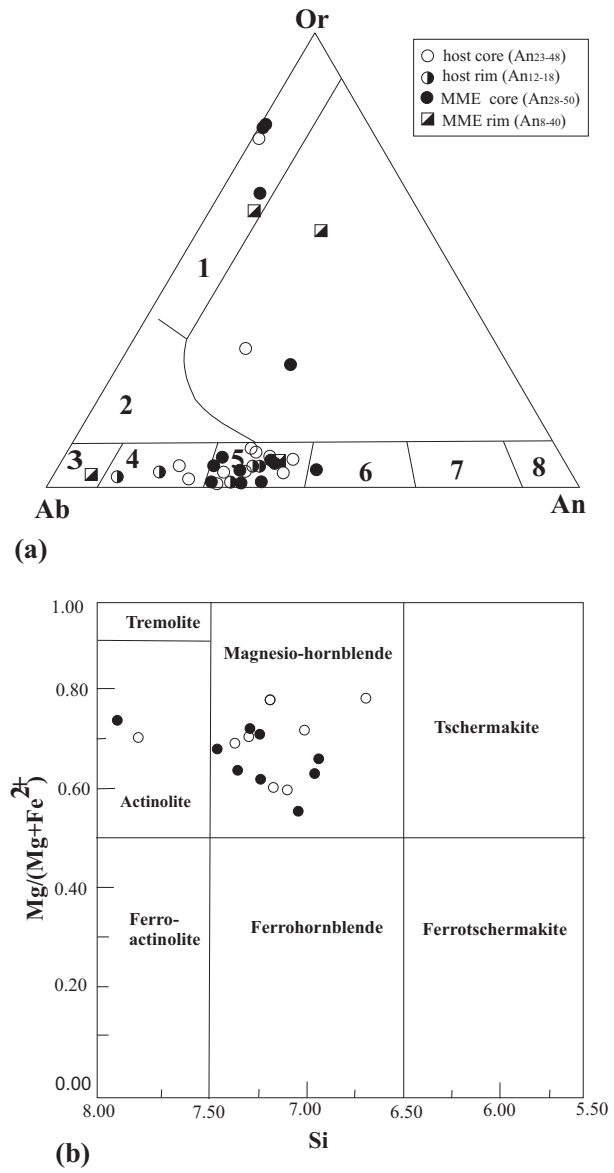

Figure 4. **(a)** Compositional variations of plagioclase from the KG and their MMEs in Ab-Or-An triangular diagram. (1) orthoclase; (2) anorthoclase; (3) albite; (4) oligoclase; (5) andesine; (6) labradorite; (7) bytownite; (8) anorthite. **(b)** Composition of amphiboles in host rocks (open circles) and their MMEs (filled circles).

1.37 with an average of 1.12, and vary from 1.01 to 1.55 with an average of 1.28, respectively. These values are similar to the Mg biotites (FeO_{tot}/MgO= 1.76), typically associated with calcic hornblende and/or pyroxene that are commonly found in calc-alkaline (mostly orogenic and subduction-related), I-type granitoid suites (Abdel-Rahman 1994). As shown in the ternary MgO-FeO_{tot}-Al_2O_3 diagram, all the biotite data from the KG and MMEs fall within the calc-alkaline orogenic suites area (Abdel-Rahman 1994; Figure 5b).

Whole Rock Geochemistry

In this chapter a joint review of the major and trace element geochemistry of the felsic host rock and the MME sample pairs, and felsic and mafic dykes is given. While felsic dykes resemble felsic host rocks, mafic rocks show similar behaviour to the MMEs in some geochemical diagrams (Tables 1–4, Figure 3).

Most KG and felsic vein rock samples and some MMEs plot in the subalkaline field, except for some MMEs and mafic vein rocks whose settings lie in the alkaline area on a total alkali (Na_2O+K_2O)-silica (SiO_2) diagram (Irvine & Baragar 1971; Figure 6a). All the samples plot in the calc-alkaline area on an AFM diagram and in the high-K field on a K_2O-SiO_2 diagram (Irvine & Baragar 1971; Le Maitre *et al.* 1989; Figure 6b, c). The KG is markedly metaluminous (mol. A/CNK<0.90) on a $Al_2O_3/(Na_2O+K_2O)$ – $Al_2O_3/(CaO+Na_2O+K_2O)$ diagram (Maniar & Piccoli 1989; Figure 6d). It displays a limited range of major element variation (59.88–67.52 % SiO_2, 1.41–2.55 % MgO, Table 1) and a monzonitic bulk composition (Figure 2). The MMEs are also metaluminous (mol. A/CNK<0.96) and similar to felsic host rocks (Table 1, Figure 6d). MMEs may be diorite, monzodiorite and quartz monzodiorite (Figure 2), include lower SiO_2 (51.76–57.97 %) and higher MgO (2.80–7.57 %) compared to KG samples. Plots of Fe_2O_3, MgO, MnO, CaO and P_2O_5 against SiO_2 contents in Harker diagrams show near-linear, negative trends in the KG, MME, felsic and mafic dykes (Figure 7b–d, g & h). It can be proposed that near-linear variations are most probably generated by the mixing of mafic and felsic magma end-members in various proportions. However, the Al_2O_3, K_2O and Na_2O contents of these rocks show that the mafic and felsic rocks define two fairly distinct trends in these diagrams (Figure 7a, b & d). Fe_2O_3 and MgO with increasing SiO_2 may partially be controlled by biotite fractionation during internal differentiation of the KG and the MME

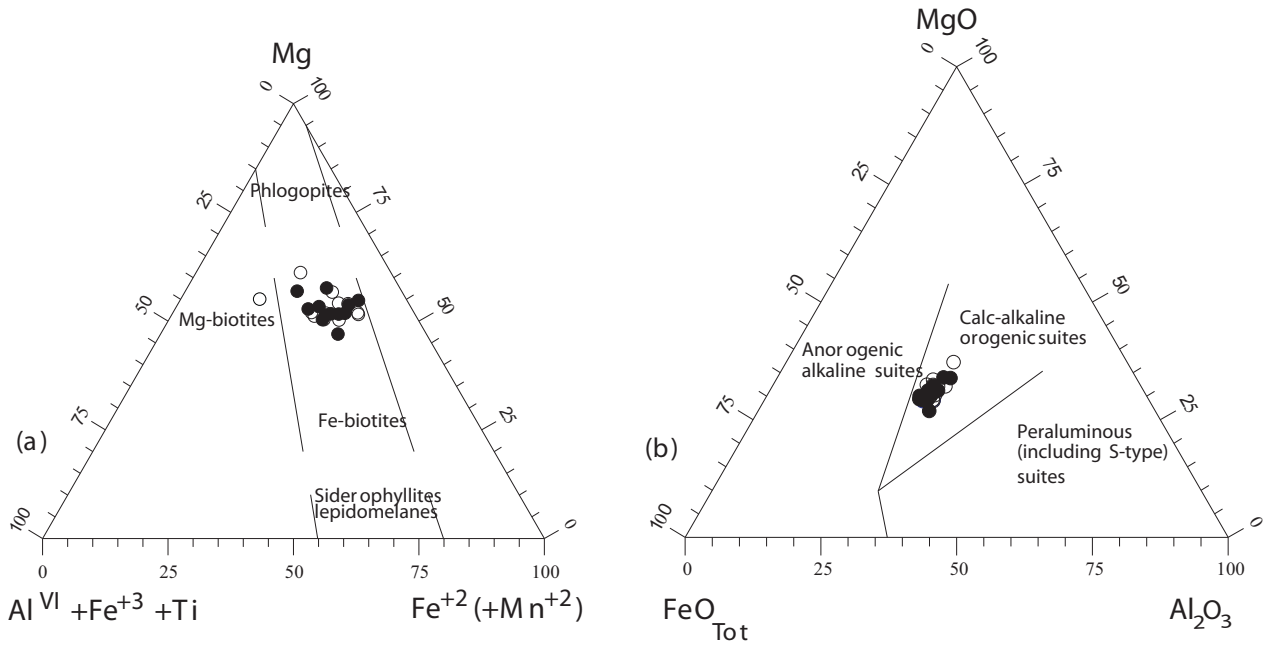

Figure 5. **(a)** Composition of biotite of the KG (open circles) and their MMEs (filled circles) in Al^{VI} + Fe^{3+} +Ti)-Mg-(Fe^{2+}+Mn) ternary diagram (Yavuz 2003a, b; after Foster 1960). **(b)** Distribution of micas of KG and MMEs on Abdel-Rahman's (1994) ternary MgO-FeO_{tot}-Al_2O_3 tectono-magmatic discrimination diagram (Yavuz 2003a, b).

magmas, coupled with a magma mixing process (Figure 7c, e). A Na_2O-SiO_2 diagrams show the increase of Na_2O content against SiO_2 which may be explained by a chemical interaction between felsic and mafic magmas (Figure 7d). On trace element (Rb, Sr, Ba,Y, Th, U, Nb, Zr) versus SiO_2 diagrams, the KG, MME and dykes have separate trends (Figure 8). The contents of some elements such as Ba, Y, Th, U, Nb and Zr, are higher in some MMEs and mafic dykes than in the felsic host and dykes. A negative corelation between Y, Zr and SiO_2 in the MME samples may result from early crystallization of Ca-rich accessory phases such as apatite and titanite, which are consistent with the observed depletion in P_2O_5 with increasing SiO_2 (Gagnevin *et al.* 2004). Rb-SiO_2 shows a regular variation (Figure 8a). U is rather high in four mafic dykes and in some MME rocks, compared to the felsic rocks. However, all the KG samples are enriched in U and especially in Th. The average U, Th and K_2O contents of the granitic samples are 12.39 ppm, 53.39 ppm and 4.64 wt%, respectively. U, Th and K_2O contents of the MMEs are 11 ppm, 29 ppm and 3.30 wt %, respectively. The activity concentrations of ^{238}U, ^{232}Th and ^{40}K in the Kestanbol granitic samples are 90.7–360.6 (average 174.78) , 110.2–340.8 (average 204.69) and 671.1–1572.3 (aver. 1171.95) Bq kg^{-1}, respectively. ^{232}Th activity concentrations are generally higher than ^{238}U in the granitic rocks. Based on these values, the Kestanbol pluton can be considered to be radioactive (Örgün *et al.* 2007). The KG-MME pairs display similar trends in MORB normalized trace element spider diagrams (Figure 9). Both show fractionation from HFS elements to LIL elements. In these diagrams, Ba, Nb and Ti are depleted, but Cs, Th, La, Nd, Sm and Gd are enriched (Figure 9a). Compared to the quartz monzonitic host on a PRIM normalised diagram, the MME displays a similar REE pattern (Taylor & McLennan 1985). Thus, it can be argued that there is a partial-to-complete equilibration between the KG and the MMEs. They exhibit enrichment in LREE relative to HREE and show discrete negative Eu anomaly. However, the negative Eu anomaly (Eu/Eu*= 0.46-0.90) was more pronounced in the MMEs than in the host rocks (Eu/Eu*= 0.61-0.84) (Tables 1 & 2, Figure 9b).

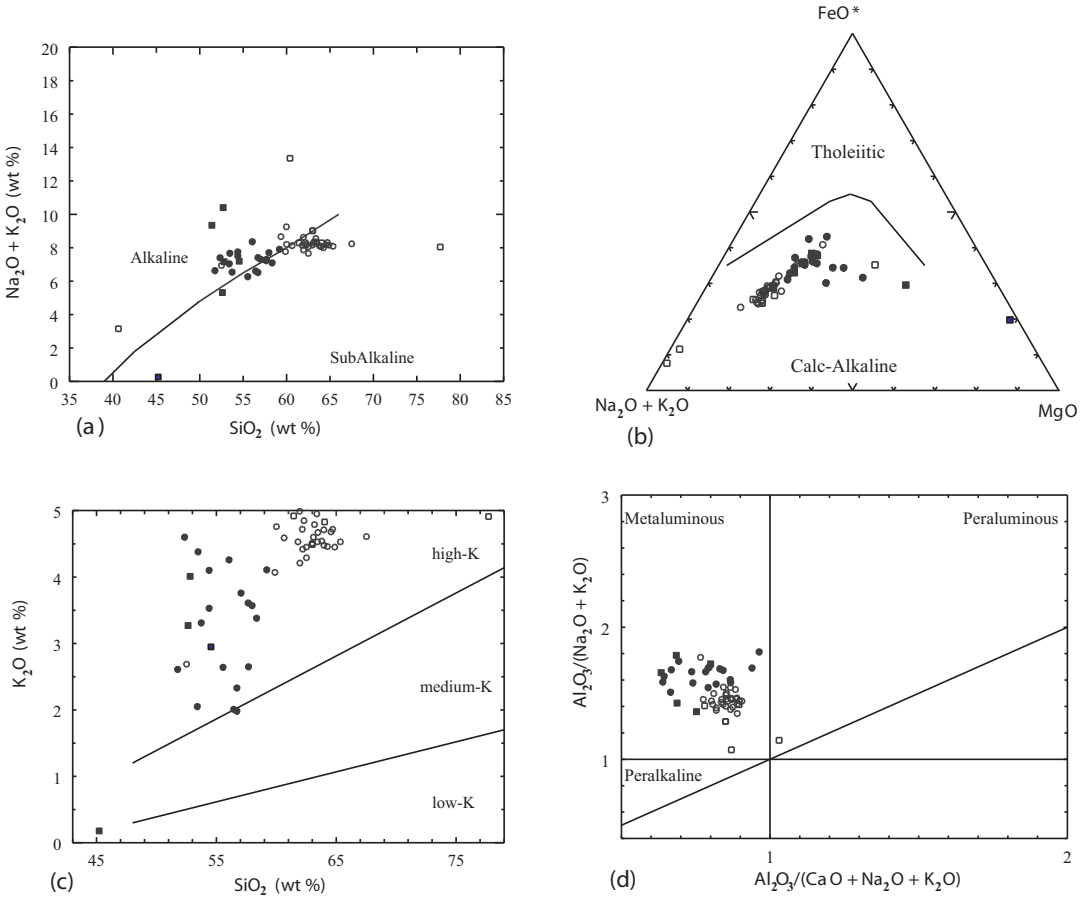

Figure 6. Plots of the samples of KG, MMEs and dykes in **(a)** total alkali versus silica diagram, **(b)** AFM diagram (Irvine & Baragar 1971), **(c)** K_2O versus silica diagram (Le Maitre *et al.* 1989), **(d)** $Al_2O3/(Na_2O+K_2O)$ versus $Al_2O_3/(CaO+Na_2O+K_2O)$ diagram (after Maniar & Piccoli 1989).

In the tectonic discrimination diagrams (Nb-Y and Rb-Y+Nb) (Pearce *et al.* 1984), most samples from the KG and MMEs plot near the Syn-COLG-WPG and VAG triple junction (Figure 10a). A few samples of the MME and mafic dykes are located in the WPG field on the Nb-Y diagram. Most samples plot in the post-collision uplift field in R1-R2 diagram (Batcheleor & Bowden 1985) but some MME and dyke rocks plot randomly elsewhere (Figure 10b). These data suggest that the KG, the MMEs and the dykes are products of post-collision magmas in western Anatolia.

Evidences of Felsic-Mafic Magma Interaction

Some of the evidence for magma mixing and mingling in the Kestanbol granitoid was determined by field and laboratory work. While the magma mingling is a characteristic of the MME zone on the map scale, magma mixing is also characterized by mixing textures on the microscopic scale.

The Kestanbol granitoid was formed by mixing of mafic magmas formed from mantle with crustal felsic material in different amounts in depths. MME, on the other hand, observed within KG may be formed in two different ways. These MMEs were produced by mingling and local mixing of mafic magma with felsic granitoid magma during their ascent and emplacement. Local mixing occurred between each blob of mafic magma and the enclosing host magma and differed from the through mixing at depth. Magma mingling can continue while the felsic magma rises and is emplaced at

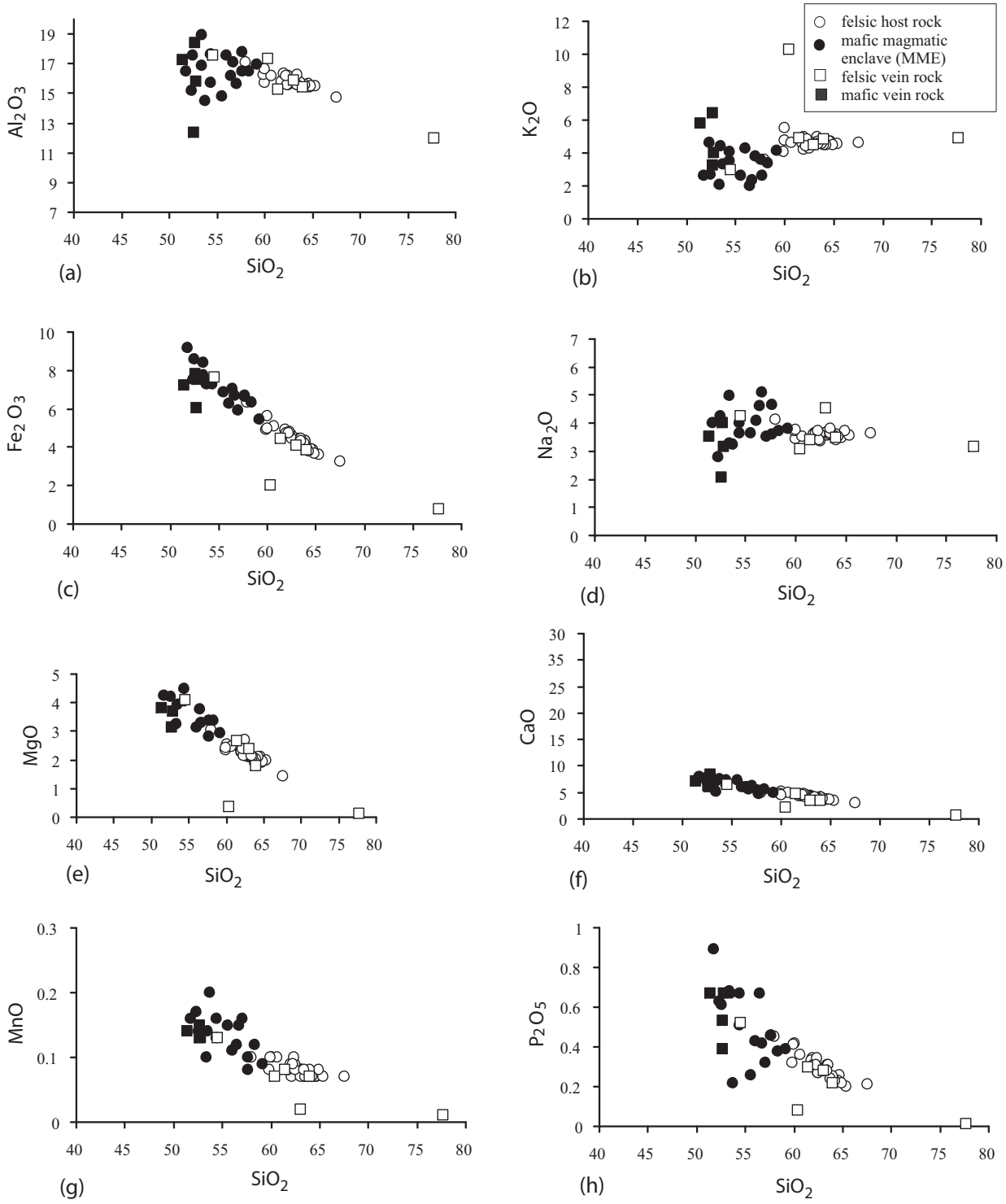

Figure 7. Harker variation diagrams for some major elements of KG, MMEs and dykes.

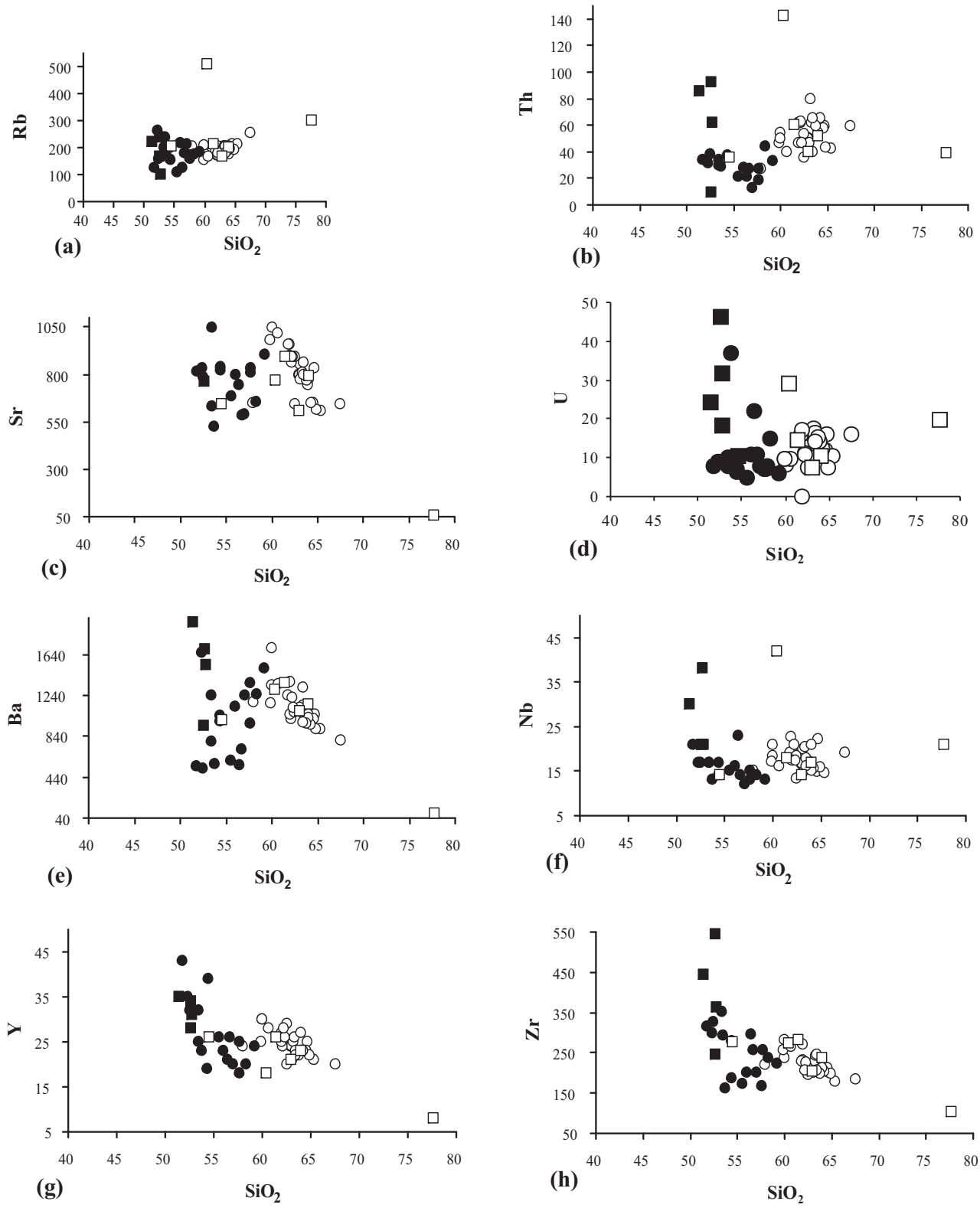

Figure 8. Harker variation diagrams for some minor elements of KG, MMEs and dykes (see Figure 7 for explanations).

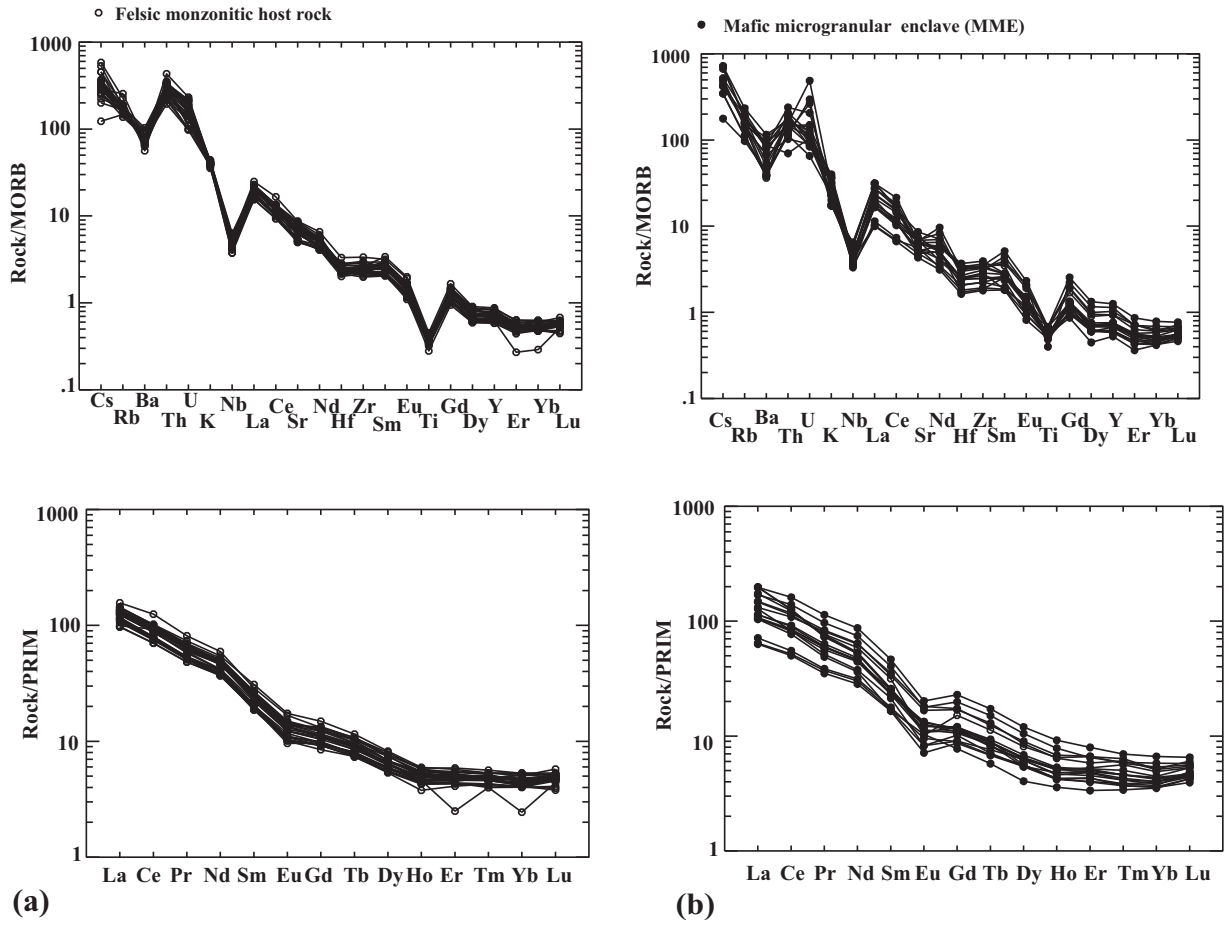

Figure 9. **(a)** MORB and **(b)** PRIM normalised diagrams of KG and MME samples (normalised values are from Taylor & McLennan 1985).

shallow depths. Simultaneously, thermal, chemical and mechanical interactions may happen between the felsic host rock and the enclaves. These interactions depend on the temperature of the mafic magmas (Kumar & Rino 2006). As a result of these interactions, some textural features, such as fine-grained, acicular and hollow minerals may form and chilled margins within felsic and mafic rocks are developed (Barbarin & Didier 1992). All of these textures can also been seen in the KG and its mafic microgranular enclaves. The magma system after thermal equilibrium may be subjected to chemical and mechanical changes (Kumar & Rino 2006). Chemical changes may occur as a result of the combination of the mafic and felsic magmas. The amount of the chemical interaction depends on the rheological properties of the felsic magma and the sizes of the MMEs. As a result of this chemical interaction, compositional convergence may occur between the KG rocks and MMEs, and after the diffusion within the enclaves, fine-grained mafic halo or more felsic halo may be seen. As a result of the mechanical interactions, on the other hand, xenocryst formation and migration of xenocrysts from one magma to another is seen. Complex crystal transfer between silicic and basic magmas is suggested by plagioclase textures and compositions (Barbarin 1990). Large plagioclase phenocrsts in the MME have a similar shape and composition to those in the monzonitic Kestanbol rocks.

The MMEs are compositionally similar to KG host rocks such as quartz monzonite, monzodiorite and diorite. Plagioclase, hornblende and biotite

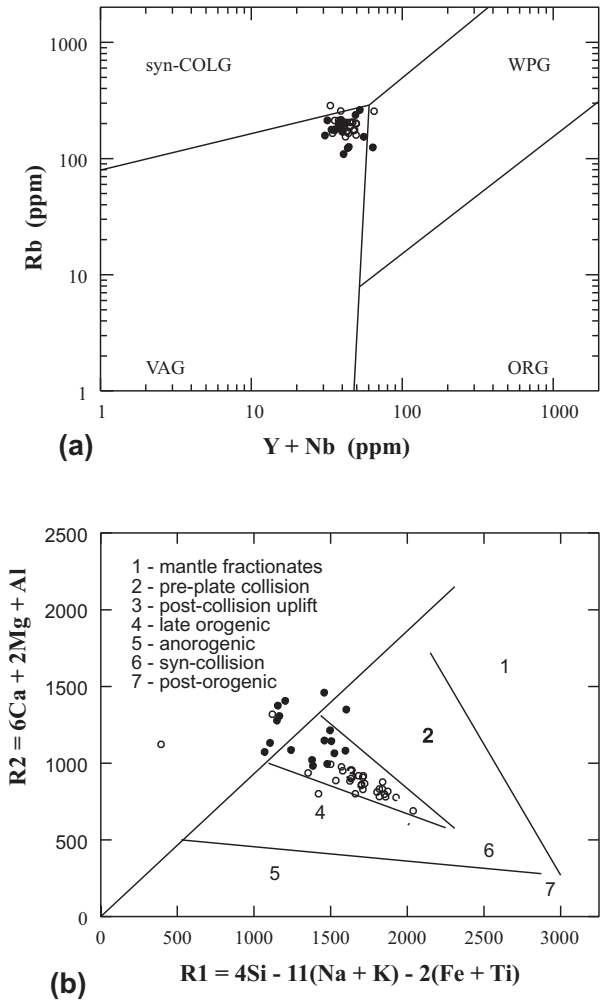

Figure 10. **(a)** Y+Nb versus Rb (Pearce *et al.* 1984) and **(b)** R1-R2 (Batcheleor & Bowden 1985) tectonic discrimination diagrams of KG and MMEs (see Figure 7 for explanations).

within the KG and the MMEs show a more or less similar range of compositions which may be re-equilibrated partly by chemical diffusion through residual melt during a syn-crystallization and mixing event in these rocks. Again, according to mineral geochemistry, plagioclase, amphibole and biotite display similar compositions in both the KG and the MMEs. Plagioclase phenocrysts in the KG and the MMEs sometimes show a cellular texture and generally have an albite-andesine composition (An_{12-50}). Amphiboles are magnesio-hornblende; biotites are Mg-biotites in composition. Orthoclase is abundantly found as elongated megacrysts in both the KG rocks and the MMEs. These megacrysts show the same flow direction as the mineral flow direction in the felsic host KG. The presence of megacrysts within the felsic and mafic magma and the fact that their longer axis are parallel to elongated enclaves show that both magmas solidified together. All these minerals are found in different proportions in the MMEs and the KG due to their co-magmatic origin. However, this feature of the MME and the KG appears to be a reflection of modal mineral re-equilibration where the MME is retained in distinctly higher modal amounts of mafic minerals, most probably during the mafic-felsic magma interaction (Kumar & Rino 2006).

We can see similar properties in MME-host rock pairs in many plutons in Turkey and also worldwide in areas such as the Central Anatolia granitoids (Kadıoğlu & Güleç 1999; Koçak 2006), the Black Sea magmatic complex (Aslan 2005; Karslı *et al.* 2004; Yılmaz Şahin 2008); Monte Capanne monzogranite (Gagnevin *et al.* 2004) and Sierra-Nevada Batholith (Barbarin 2005). These characteristic similarities can be verified by isotope data.

Conclusions

Coeval mafic and felsic magmas formed the MME hosted in the Miocene, high-K calc-alkaline Kestanbol granitoid by magma mixing, mingling and thermal, mechanical and chemical interaction processes leading to different degrees of re-equilibration between the MME and the KG. According to geochemistry of amphibole minerals, the KG formed under 1.17–3.6 Kbar pressure, and 659–799 °C temperature, whereas MME samples formed at 1.24–3.84 Kbar and 692–766 °C. Mg-biotites, common in both the KG and the MME, reflect the calc-alkaline, orogenic, I-type granitoids character.

The KG and its MMEs show near-similar trends in some geochemical diagrams which mostly evolved and because they interacted with each other chemically. The major element geochemistry of the KG indicates a metaluminous, subalkaline, I-type and high-K calc-alkaline character with intermediate SiO_2 (59.88–67.52 wt%), high K_2O (4.07–5.41 wt%), middle Na_2O (3.37–3.71 wt%) and Middle Al_2O_3

(14.75–16.24 wt%). The MMEs have SiO_2 (51.76–59.19 wt%), high K_2O (2.05–4.60 wt%), middle Na_2O (2.80–5.08 wt%), middle Al_2O_3 (14.49–18.91 wt%). The molecular A/CNK ratios of the Kestanbol pluton's samples range from 0.77 to 0.90 whereas the range in MMEs is 0.64–0.94. The Kestanbol pluton and its MMEs show a slightly negative Eu anomaly (EuN/Eu*= 0.61–0.84 and 0.46–0.90), respectively.

All the mineralogical, petrographical and geochemical data suggest that the MME, syn-plutonic dykes and mafic dykes were formed in the advanced stages of crystallization of the hybrid Kestanbol granitoid host magma.

Acknowledgement

This study is financially supported by The Scientific and Technological Research Council of Turkey (TÜBİTAK) (Project number: 104Y031). The authors are thankful to Çekmece Nuclear Research and Training Center (ÇNAEM) for support and cooperation. We also thank Dr. Fuat Yavuz for determination of mineral chemistry results. The authors thank Dr. Yusuf Kaan Kadıoğlu for his helpful and constructive reviews and Dr. Erdin Bozkurt for his editorial handling of the manuscript. John A. Winchester edited English of the final text.

References

Abdel-Rahman, A.M. 1994. Nature of biotites from alkaline, calc-alkaline, and peraluminous magmas. *Journal of Petrology* **35**, 525–541.

Aldanmaz, E. 2006. Mineral-chemical constraints on the Miocene calc-alkaline and shoshonitic volcanic rocks of Western Turkey: disequilibrium phenocryst assemblages as indicators of magma storage and mixing conditions. *Turkish Journal of Earth Science* **15**, 47–73.

Andaç, M. 1973. *Biga Yarımadasında Ezine Siyenit Masifi ile Civarındaki Kayaçların Petrografisi ve Bu Kayaçlardan Meydana Gelen Radyoaktif Sahil Plazer Maden Yatağının Etüdü [Petrography of Ezine Syenite Massif and Rocks Around it in Biga Peninsula: Exploration of Radioactive Beach Placers Originated from These Rocks]*. İstanbul Technical University, DSc Thesis [in Turkish with English abstract, unpublished].

Aslan, Z. 2005. Petrography and petrology of the calc-alkaline Sarıhan granitoid (NE Turkey): an example of magma mingling and mixing. *Turkish Journal of Earth Sciences* **14**, 185–207.

Barbarin, B. 1988. Field evidence for successive mixing and mingling between the Pioland Diorite and the Saint Julien –la-Vetre Monzogranite (Nord Fore, Massif Central, France). *Canadian Journal of Earth Sciences* **25**, 49–59.

Barbarin, B. 1990. Plagioclase xenocrysts and mafic magmatic enclaves in some granitoids of the Sierra Nevada Batholith, California. *Journal of Geophysical Research* **95**, 17747–17756.

Barbarin, B. 1999. A review of the relationships between granitoid types, their origins and their geodynamic environments. *Lithos* **46**, 605–626.

Barbarin, B. 2005. Mafic magmatic enclaves and mafic rocks associated with some granitoids of the central Sierra Nevada batholith, California: nature, origin, and relations with the hosts. *Lithos* **80**, 155–177.

Barbarin, B. & Didier, J. 1992. Genesis and evolution of mafic microgranular enclaves through various types of interaction between coexisting felsic and mafic magmas. *Transactions of the Royal Society of Edinburgh Earth Sciences* **83**, 145–153.

Batcheleor, B. & Bowden, P. 1985. Petrogenetic ınterpretation of granitoid rock series using multicationic parameters. *Chemical Geology* **48**, 43–55.

Birkle, P. & Satir, M. 1992. Petrology, geochemistry and geochranology of a quartz-monzonite intrusion (Kestanbol granite) and their host rocks near Ezine, Biga-peninsula, NW Anatolia, Turkey. *ISGB-92 Abstracts,* 44–45.

Blundy, J.D. & Holland, T.J.B. 1990. Calcic amphibole equilibria and a new amphibole-plagioclase geothermometer. *Contributions to Mineralogy and Petrology* **104**, 208–224.

Debon, F. & Le Fort, P. 1983. A chemival-mineralogical classification of common plutonic rocks and associations. *Transactions of the Royal Society of Edinburgh Earth Sciences* **73**, 135–149.

Delaloye, M. & Bingöl, E. 2000. Granitoids from Western and Northwestern Anatolia: geochemistry and modeling of geodynamic evolution. *International Geology Rewiev* **42**, 241–268.

Didier, J. & Barbarin, B. (eds) 1991. *Enclaves and Granite Petrology: Developments in Petrology 13*. Elsevier, Amsterdam.

Fernandez, A.N. & Barbarin, B. 1991. Relative rheology of coeval mafic and felsic magmas: nature of resulting interaction processes. Shape and mineral fabrics of mafic microgranular enclaves. *In*: Didier, J. & Barbarin, B. (eds), *Enclaves and Granite Petrology: Developments in Petrology* 13. Elsevier, 263–275.

Foster, M.D. 1960. *Interpretatıon of the Composition of Trioctahedral Micas*. United States Geological Survey Prefessional Paper **354-B**, 11–49.

Gagnevin, D., Daly, J.S. & Poli, G. 2004. Petrographic, geochemical and isotopic constraints on magma dynamics and mixing in the Miocene Mont Capanne monzogranite (Elba Island, Italy). *Lithos* **78**, 157–195.

Hibbard, M.J. 1991. Textural anatomy of twelve magma mixed granitoid systems. *In*: Didier, J. & Barbarin, B. (eds), *Enclaves and Granite Petrology: Development in Petrology 13*. Elsevier, Amsterdam, 431–444.

Hibbard, M.J. 1995. *Petrography to Petrogenesis*. Prentice Hall.

Irvine, T.N & Baragar, W.R.A. 1971. A guide to the chemical classification of common volcanic rocks. *Canadian Journal of Earth Sciences* **8**, 523–548.

Kadioğlu, Y.K & Güleç, N. 1999. Types and genesis of the enclaves in Central Anatolian granitoids. *Geological Journal* **34**, 243–256.

Karacik, Z. 1995. *Ezine-Ayvacık (Çanakkale) Dolayında Genç Volkanizma-plütonizma İlişkileri [Relationship Between Young Volcanism and Plutonism in Ezine-Ayvacık (Çanakkale) Region]*. PhD Thesis, İstanbul Technical University [in Turkish with English abstract, unpublished].

Karacik, Z. & Yilmaz, Y. 1998. Geology of ignimbrites and the associated volcano-plutonic complex of the Ezine area, northwestern Anatolia. *Journal of Volcanology and Geothermal Research* **85**, 251–264.

Karsli, O., Aydin, F & Sadiklar, B. 2004. The morphology and chemistry of K-feldspar magacrysts from İkizdere Pluton: evidence for acid and basic magma interactions in granitoid rocks, NE-Turkey. *Chemie der Erde* **64**, 155–170.

Koçak, K. 2006. Hybridization of mafic microgranular enclaves: mineral and whole-rock chemistry evidence from the Karamadazı Granitoid, Central Turkey. *International Journal of Earth Sciences* **95**, 597–607.

Kumar, S. & Rino, V. 2006. Mineralogy and geochemistry of microgranular enclaves in Palaeoproterozoic Malanjkhand granitoids, central India: evidence of magma mixing, mingling, and chemical equilibration. *Contributions to Mineralogy and Petrology* **152**, 591–609.

Le Maitre, R.W., Bateman, P., Dudek, A., Keller, J., Lameyre, J., Le Bas, M.J., Sabine, P.A., Schmid, R., Sorensen, H., Streckeisen, A., Woodley, A.R & Zanettin, B. 1989. *A Classification of Igneous Rocks and Glossary of Terms*. Recommendations of the International Union of Geological Sciences Subcommission of the Systematics of Igneous Rocks. Blackwell Scientific Publications.

Leake, B.E., Wooley, A.R., Arps, C.E.S., Birch, W.D., Gilbert, M.C., Grice, J.D., Hawthorne, F.C., Kato, A., Kisch, H.J., Krivovichev, V.G., Linhout, K., Laird, J., Mandaring, J.A., Maresch, W.V., Nickel, E.H., Rock, N.M.S., Schumacher, J.C., Smith, D.C., Stephenson, N.C.N., Ungaretti, L., Whittaker, E.J.W. & Youzhi, G. 1997. Nomenclature of Amphiboles. Report of the Subcommittee on Amphiboles of the International Mineralogical Association, Commission on New Minerals and Mineral Names. *Canadian Mineralogist* **35**, 219–246.

Maniar, P.D. & Piccoli, P.M. 1989. Tectonic discrimination of granitoids. *Geological Society of America Bulletin* **101**, 635–643.

Okay, İ.A. & Satir, M. 2000. Coeval plutonism and metamorphism in a latest Oligocene metamorphic core complex in northwest Turkey. *Geological Magazine* **137**, 495–516.

Örgün, Y., Altinsoy, N., Yilmaz Şahin, S., Güngör, Y., Gültekin, A.H., Karahan, G. & Karacik, Z. 2007. Natural and anthropogenic radionuclides in rocks and beach sands from Ezine region (Çanakkale). Western Anatolia, Turkey. *Applied Radiation and Isotopes* **65**, 739–747.

Pearce, J.A., Harris, N.B.W & Tindle, A.G. 1984. Trace element discrimination diagrams for the tectonic interpretion of granitic rocks. *Journal of Petrology* **25**, 956–983.

Taylor, S.R. & McLennan, S.M. 1985. *The Continental Crust: its Composition and Evolution*. Blackwell, Oxford.

Vernon, R.H. 1986. K-feldspar megacrysts in granites – phenocrysts, not porphyroblasts. *Earth-Science Reviews* **23**, 1–63.

Vernon, R.H., Etheridge, M.A & Wall, V.J. 1988. Shape and microstructure of granitoid enclaves: indicators of magma mingling and flow. *Lithos* **22**, 1–11.

Yavuz, F. 2003a. Evaluating micas in petrologic and metallogenic aspect: I- definitions and structure of the computer program MICA+. *Computers & Geosciences* **29**, 1203–1213.

Yavuz, F. 2003b. Evaluating micas in petrologic and metallogenic aspect: II- Applications using the computer program MICA+. *Computers & Geosciences* **29**, 1215–1228.

Yavuz, F. 2007. WinAmphcal: A windows program for the IMA-04 amphibole classification. *Geochemistry Geophysics Geosystems* 8, Q01004, doi:10. 1029/2006GC001391.

Yilmaz, Y. 1997. Geology of Western Anatolia: active tectonics of northwestern Anatolia. *The Marmara Poly Project. VDF, Hochschulverlag Ag An Der ETH*, Zürich 1–20.

Yilmaz, Y., Genç, Ş.C., Karacik, Z & Altunkaynak, S. 2001. Two contrasting magmatic associations of NW Anatolia and their tectonic significance. *Journal of Geodynamics* **31**, 243–271.

Yilmaz, S. & Boztuğ, D. 1994. Granitoyid petrojenezinde magma mingling/mixing kavramı: Türkiye'den bazı örnekler [The concept of magma mingling/mixing in granitoid petrogenesis: examples from Turkey]. *Jeoloji Mühendisliği* **44-45**, 1–20 [in Turkish with English abstract].

Yilmaz Şahin, S., Güngör, Y & Göker, F.A. 2004. Macroscopical and microscopical evidences magma mixing/mingling type interaction of in Kestanbol granitoid (South Çanakkale), Northwest Anatolia-Turkey. *4th International Scientific Conference, Modern Management of Mine Producing, Geology and Environmental Protection, SGEM 2004, Bulgaria, Proceeding*, 3–14.

Yilmaz Şahin, S. 2008. Geochemistry of mafic microgranular enclaves in The Tamdere quartz monzonite, South of Dereli/Giresun, eastern Pontides, Turkey. *Chemie der Erde – Geochemistry* **68**, 81–92.